## Title

Loss of Apc Cooperates with Activated Oncogenes to Induce Liver Tumor Formation in Mice



## Journal

American Journal Of Pathology, 191(5)

## ISSN

0002-9440

## Authors

Zhang, Yi
Liang, Binyong
Song, Xinhua
et al.

## Publication Date

2021-05-01

## DOI

10.1016/j.ajpath.2021.01.010

Peer reviewed

The American Journal of Pathology, Vol. 191, No. 5, May 2021

ELSEVIER

The American Journal of PATHOLOGY

ajp.amjpathol.org

TUMORIGENESIS AND NEOPLASTIC PROGRESSION

# Loss of Apc Cooperates with Activated Oncogenes to Induce Liver Tumor Formation in Mice



Yi Zhang,*† Binyong Liang,‡ Xinhua Song,† Haichuan Wang,§¶ Matthias Evert,‖ Yi Zhou,** Diego F. Calvisi,‖ Liling Tang,* and Xin Chen†,††

*From the Key Laboratory of Biorheological Science and Technology,* Ministry of Education, College of Bioengineering, Chongqing University, Chongqing, China; the Department of Bioengineering,† University of California, San Francisco, San Francisco, California; the Hepatic Surgery Center,‡ Department of Surgery, Tongji Hospital, Tongji Medical College, Huazhong University of Science and Technology, Wuhan, China; the Liver Transplantation Division,§ Department of Liver Surgery, and the Laboratory of Liver Surgery,¶ West China Hospital, Sichuan University, Chengdu, Sichuan, China; Institute of Pathology,‖ University of Regensburg, Regensburg, Germany; Department of Infectious Diseases,** The First Affiliated Hospital of Xi'an Jiaotong University, Xi'an, China; and the Department of Therapeutic Sciences and Liver Center,†† University of California, San Francisco, San Francisco, California*

Accepted for publication January 14, 2021.

Address correspondence to Liling Tang, Ph.D., Key Laboratory of Biorheological Science and Technology, Ministry of Education, College of Bioengineering, Chongqing University, 174 Shazhengjie, Shapingba, Chongqing 400044, China; or Xin Chen, Ph.D., Department of Bioengineering and Therapeutic Sciences, University of California, San Francisco, 513 Parnassus Ave., HSE1420, San Francisco, CA 94143. E-mail: tangliling@cqu.edu.cn or xin.chen@ucsf.edu.

Hepatocellular carcinoma (HCC) and hepatoblastoma are the major types of primary liver cancer in adulthood and childhood, respectively. Wnt/β-catenin signaling deregulation is one of the most frequent genetic events in hepatocarcinogenesis. APC regulator of WNT signaling pathway (*APC*) encodes an inhibitor of the Wnt cascade and acts as a tumor suppressor. Germline defects of the *APC* gene lead to familial adenomatous polyposis, and its somatic mutations occur in multiple tumor types. However, the contribution of APC in hepatocarcinogenesis remains unclear. Therefore, *APC* mutations and expression patterns were examined in human HCC and hepatoblastoma samples. Whether loss of Apc alone or in cooperation with other oncogenes triggers liver tumor development *in vivo* was also investigated. sgApc alone could not drive liver tumor formation, but synergized with activated oncogenes (YapS127A, TazS89A, and c-Met) to induce hepatocarcinogenesis. Mechanistically, Apc deletion induced the activation of β-catenin and its downstream targets in mouse liver tumors. Furthermore, *Ctnnb1* ablation or TCF4-mediated transcription blockade completely prevented liver tumor formation, indicating the requirement of a functional β-catenin pathway for loss of Apc-driven hepatocarcinogenesis. This study shows that a subset of HCC patients with loss-of-function *APC* mutations might benefit from therapeutic strategies targeting the Wnt/β-catenin pathway. *(Am J Pathol 2021, 191: 930–946; https://doi.org/10.1016/j.ajpath.2021.01.010)*

Primary liver cancer is the sixth most common cancer worldwide, with approximately 800,000 new cases each year.[1] Hepatocellular carcinoma (HCC) and hepatoblastoma (HB) are the two prevalent primary liver malignancies derived from mature hepatocytes or hepatic progenitor cells.[2] HCC is the most common primary hepatic malignancy in adults and accounts for more than 80% of liver cancer cases.[3] Due to its late diagnosis, high mortality rate, and rising incidence, HCC is a major health concern globally.[4] HB is the most common pediatric liver malignancy. It is thought to arise from hepatic progenitor cells undergoing malignant transformation during embryogenesis.[2] The common histologic HB subtypes are epithelial, mesenchymal, fetal, and embryonal. Tumors in patients with HB rarely consist of only one cell type, usually exhibiting the combinations of epithelial, mesenchymal, and other histologic components.[5] Despite the growing incidence of primary liver cancer, treatment options are extremely limited for the affected patients, especially for HCC.[4] On the other hand, most patients with HB can be effectively treated, but the aggressive therapies severely and negatively affect their quality of life.[5] Thus, there is an urgent need to unravel

Supported by NIH grants R01CA204586 (X.C.), R01CA250227 (X.C.), and P30DK026743 (UCSF Liver Center).

Disclosures: None declared.


https://doi.org/10.1016/j.ajpath.2021.01.010

**Table 1** Primary Antibodies for IHC

| Antibody | Species | Dilution | Company | Catalog no. |
|---|---|---|---|---|
| Ki-67 | Rabbit | 1:150 | Cell Signaling Technology (Danvers, MA) | 12202 |
| APC | Rabbit | 1:100 | Abcam (Cambridge, MA) | Ab40778 |
| β-Catenin | Mouse | 1:200 | BD Biosciences (San Jose, CA) | 610153 |
| YAP | Rabbit | 1:100 | Cell Signaling Technology | 14074 |
| TAZ | Mouse | 1:200 | BD Biosciences | 560235 |
| c-Met | Rabbit | 1:100 | Abcam | Ab51067 |
| HNF4α | Rabbit | 1:500 | Abcam | Ab181604 |
| CEBPα | Rabbit | 1:500 | Cell Signaling Technology | 8178 |
| SOX9 | Rabbit | 1:400 | Cell Signaling Technology | 82630 |
| CK7 | Rabbit | 1:500 | Abcam | Ab181598 |
| GLUL | Mouse | 1:500 | BD Biosciences | 610518 |
| CK19 | Rabbit | 1:200 | Abcam | Ab133496 |
| FASN | Mouse | 1:500 | BD Biosciences | 610962 |
| SCD1 | Rabbit | 1:200 | Cell Signaling Technology | 2794 |
| p-mTOR-Ser2448 | Rabbit | 1:100 | Cell Signaling Technology | 2976 |

IHC, immunohistochemistry

the molecular mechanisms of HCC and HB tumorigenesis for the development of effective targeted therapies against these aggressive diseases.

The Wnt/β-catenin signaling is an evolutionarily conserved cascade, representing one of the key pathways controlling cell proliferation, differentiation, and survival.[6,7] In the liver, the Wnt/β-catenin cascade regulates a plethora of events, including hepatocyte development, and liver metabolism, regeneration, and homeostasis.[8] Thus, it is not surprising that alterations in this pathway lead to numerous liver diseases, including cancer. In both HCC and HB, the Wnt/β-catenin pathway is commonly hyperactivated. Moreover, frequent mutations in some key components of the Wnt pathway have been detected in the two tumor entities, with catenin beta-1 (*CTNNB1*) being the most frequently mutated gene. *CTNNB1* encodes β-catenin, the essential molecular effector of the Wnt cascade. Most of the *CTNNB1* mutations are deletions or missenses substitutions at the glycogen synthase kinase-3β phosphorylation motif of β-catenin, resulting in constitutive activation of β-catenin. Gain-of-function (GOF) mutations in *CTNNB1* occur in approximately 15% to 30% of human HCCs[8] and in almost 80% of HB samples.[9] In addition to *CTNNB1*-activating mutations, loss-of-function (LOF) mutations in some components of the β-catenin destruction complex, such as *AXIN1* and *APC*, have been found in HCC and HB.[8,10]

APC is a well-known tumor suppressor. It binds to and enhances GSK-3β activity to facilitate β-catenin phosphorylation and subsequent degradation.[11] Germline mutations of *APC* lead to familial adenomatous polyposis,[12] an autosomal dominant inherited condition associated with a high risk of developing colorectal adenomas and hepatic tumors, including HB and HCC.[13,14] In particular, compared with the general population, patients with familial adenomatous polyposis parental history or diagnosed with familial adenomatous polyposis have approximately 400 to 800 times higher risk of developing HB.[15,16] Somatic LOF mutations in *APC* are frequently detected in colorectal, gastric, and pancreatic tumors.[17–19] In primary liver cancer, LOF *APC* mutations are detected in approximately 3% of HCCs and 20% of HBs (COSMIC, *https://cancer.sanger.ac.uk/cosmic*, last accessed December 25, 2020). In HCCs, LOF mutations in *APC* trigger the activation of the WNT/β-catenin signaling cascade.[20] *APC* somatic mutant HCCs are related to etiologies such as hepatitis B virus infection.[21] In patients with *APC* germline mutations (called APC-HB), HB lesions exhibit the activation of the Wnt signaling pathway.[22] In the clinical setting, *APC*-inactivating mutations in HB promote cisplatin-induced tertiary lymphoid structures, which initiate the immune response and contribute to a more favorable prognosis.[22]

**Table 2** Primary Antibodies Used for Western Blot Analysis

| Antibody | Species | Dilution | Company | Catalog no. |
|---|---|---|---|---|
| YAP/TAZ | Rabbit | 1:1000 | Cell Signaling Technology | 8418 |
| APC | Rabbit | 1:500 | Thermo Fisher Scientific | PA530580 |
| β-Catenin | Mouse | 1:1000 | BD Biosciences | 610153 |
| GS | Mouse | 1:5000 | BD Biosciences | 610518 |
| NOTCH2 | Rabbit | 1:10,000 | Cell Signaling Technology | 5732 |
| JAG-1 | Rabbit | 1:1000 | Abcam | Ab109536 |
| SOX9 | Rabbit | 1:5000 | Abcam | Ab185230 |
| GAPDH | Mouse | 1:10,000 | EMD Millipore (Burlington, MA) | AB2302 |

**Table 3** Primer Sequences Used for Quantitative Real-Time RT-PCR Analysis

| Gene | Forward | Reverse |
|---|---|---|
| 18s rRNA | 5′-CGGCTACCACATCCAAGGAA-3′ | 5′-GCTGGAATTACCGCGGCT-3′ |
| *Myc* | 5′-TGTACCTCGTCCGATTCC-3′ | 5′-CATCTTCTTGCTCTTCTTCAG-3′ |
| *Ccnd1* | 5′-CGTGGCCTCTAAGATGAAGGA-3′ | 5′-CCTCGGGCCGGATAGAGTAG-3′ |
| *Axin2* | 5′-GCTCCAGAAGATCACAAAGAGC-3′ | 5′-AGCTTTGAGCCTTCAGCATC-3′ |
| *Lgr5* | 5′-ACCGAGCCTTACAGAGCCT-3′ | 5′-GCCGTCGTCTTTATTCCATTGG-3′ |
| *Lect2* | 5′-CCCACAACAATCCTCATTTCAGC-3′ | 5′-ACACCTGGGTGATGCCTTTG-3′ |
| *Glul* | 5′-CAGGCTGCCATACCAACTTCA-3′ | 5′-TCCTCAATGCACTTCAGACCAT-3′ |
| *Tbx3* | 5′-CAGGCAGCCTTCAACTGCT-3′ | 5′-GGACACAGATCTTTGAGGTTGGA-3′ |
| *Sp5* | 5′-AGGACAGGAAACTGGGTCGT-3′ | 5′-GATGGCTCGGACTTTGGA-3′ |
| *Ccn2* | 5′-GGGCCTCTTCTGCGATTTC-3′ | 5′-ATCCAGGCAAGTGCATTGGTA-3′ |
| *Ccn1* | 5′-CTGCGCTAAACAACTCAACGA-3′ | 5′-GCAGATCCCTTTCAGAGCGG-3′ |
| *Notch2* | 5′-ATGTGGACGAGTGTCTGTTGC-3′ | 5′-GGAAGCATAGGCACAGTCATC-3′ |
| *Jag1* | 5′-CCTCGGGTCAGTTTGAGCTG-3′ | 5′-CCTTGAGGCACACTTTGAAGTA-3′ |
| *Hes1* | 5′-AAAGCCTATCATGGAGAAGAGGCG3′ | 5′-GGAATGCCGGGAGCTATCTTTCTT-3′ |
| *Hey1* | 5′-GCGCGGACGAGAATGGAAA-3′ | 5′-TCAGGTGATCCACAGTCATCTG-3′ |
| *Afp* | 5′-TCTGCTGGCACGCAAGAAG-3′ | 5′-TCGGCAGGTTCTGGAAACTG-3′ |
| *Gpc3* | 5′-CAGCCCGGACTCAAATGGG-3′ | 5′-CAGCCGTGCTGTTAGTTGGTA-3′ |
| *Epcam* | 5′-GCGGCTCAGAGAGACTGTG-3′ | 5′-CCAAGCATTTAGACGCCAGTTT-3′ |

In the liver, the Hippo signaling pathway has an essential role in controlling liver size and regeneration, as well as in tumorigenesis.[23] Yes-associated protein (YAP) and its paralog transcriptional coactivator with a PDZ-binding motif (TAZ) are the major transcriptional coactivators downstream of Hippo kinases.[24] When the Hippo pathway is turned on, YAP/TAZ are phosphorylated by the Hippo kinases, resulting in their cytoplasmic sequestration and proteasomal degradation.[24] When the Hippo pathway is turned off, dephosphorylated YAP/TAZ translocate into the nucleus and interact with DNA-binding transcription factors, mainly TEADs, to activate target gene expression.[25] Dysregulation of the Hippo pathway and YAP/TAZ activation are commonly observed in HCC and HB.[26–28]

Activation of c-Met is another important signaling event in HCC.[29,30] The c-Met tyrosine kinase receptor is expressed on the plasma membrane of the hepatocytes.[31] The dimerization and activation of c-Met through binding with one known ligand, hepatocyte growth factor, leads to the stimulation of multiple signaling pathways.[32] Among them, the phosphatidylinositol 3-kinase/AKT and the rat sarcoma virus/extracellular signal-regulated kinase cascades execute the cellular effects of c-Met activation to regulate hepatocyte proliferation and survival.[33,34] Aberrant c-Met activation occurs in approximately 50% of HCCs, where it is associated with poor prognosis in patients.[33,35,36]

In the present study, the mutation frequency and expression levels of APC in human HCC and HB samples were systematically analyzed. Whether loss of Apc, either alone or in combination with overexpression of additional proto-oncogenes, including Yap, Taz, or c-Met, is able to promote liver tumor development in mice, was investigated. The data obtained show that LOF *APC* mutations are present in a small subset of human HCC samples, in which targeting β-catenin may offer an effective treatment.

## Materials and Methods

### Constructs and Reagents

The plasmids used in this study for mouse injection, including pT3-EF1α-YapS127A, pT3-EF1α-TazS89A, pT3-EF1α-c-Met, pX330-sgApc, pT3-EF1α-ΔN90-β-catenin, pCMV, pCMV-Cre, pCMV-Sleeping Beauty transposase (pCMV/SB), pT3-EF1α, and pT3-EF1α-dnTCF4, were previously described.[37–41] The pX330-sgApc plasmid was kindly provided by Dr. Wen Xue (University of Massachusetts Medical School, Worcester, MA). All plasmids were extracted using the Endotoxin-Free Maxiprep kit (Sigma-Aldrich, St. Louis, MO).

### Mice and Hydrodynamic Tail Vein Injection

FVB/N mice and *Ctnnb1*$^{f/f}$ (on a C57Bl6 background) mice were used for this study. All mice were purchased from the Jackson Laboratory (Sacramento, CA). Five- to 7-week–old mice (body weight of 20 g) were subjected to plasmid injection. Mice were injected with saline solution plus the plasmid mixture, equivalent to 10% of body weight, via hydrodynamic tail vein injection in combination with Sleeping Beauty–mediated somatic integration as described in our previous study.[42] FVB/N mice were injected with plasmids at the following doses: Yap (20 μg)/sgApc (20 μg), Yap (20 μg)/βcatenin (20 μg), sgApc (20 μg), Yap (20 μg)/sgApc (20 μg)/pT3 (60 μg), and Yap (20 μg)/sgApc (20 μg)/dnTCF4 (60 μg). *Ctnnb1*$^{f/f}$ mice were injected with plasmids at the following doses: Yap (20 μg)/sgApc (20 μg)/pCMV (60 μg) and Yap (20 μg)/sgApc (20 μg)/Cre (60 μg). All the plasmids were mixed with pCMV/Sleeping Beauty transposase (pCMV/SB) in a 25:1 ratio and then delivered into the mice. Mice were kept and monitored according to the protocols

**A**

| Dataset | HCC cases, *n* | Mutated cases, *n* | % Mutated |
|---|---|---|---|
| TCGA | 372 | 12 | 3.2% |
| MSK | 127 | 7 | 5.5% |
| INSERM | 243 | 3 | 1.2% |
| AMC | 231 | 4 | 1.7% |
| COSMIC | 1091 | 31 | 2.84% |
| **Total** | **2064** | **57** | **2.76%** |

**B**

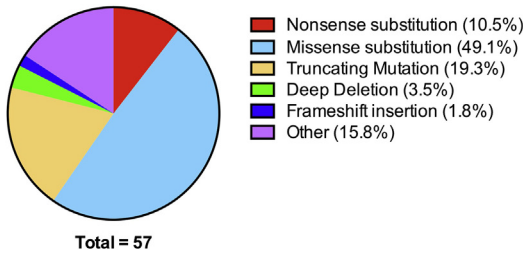


**Figure 1** *APC* mutations in human hepatocellular carcinoma (HCC) samples. **A:** Analysis of *APC* mutations in human HCC samples based on the TCGA LIHC, MSK, INSERM, AMC, and COSMIC databases. **B:** Overview of the types of *APC* mutations observed in human HCC samples.

approved by the Committee for Animal Research at the University of California, San Francisco.

## Histology and Immunohistochemistry

Mouse liver tissues were fixed in 10% Neutral Buffered Formalin (Thermo Fisher Scientific, Waltham, MA) at 4°C overnight and then processed for paraffin embedding. Mouse liver tissue sections were cut at 5-μm thickness by tissue slicer (Leica RM 2155; Leica Microsystems, Wetzlar, Germany) and used for hematoxylin and eosin (H&E; Thermo Fisher Scientific) staining and immunohistochemistry (IHC). For H&E staining, sections were stained according to the standard protocol. For IHC, sections were deparaffinized in xylene and hydrated in a series of graded alcohols, and then boiled in 10 mmol/L sodium citrate buffer (pH 6.0) for 10 minutes for antigen retrieval. After cooling down at room temperature, sections were blocked in 10% goat serum and Avidin/Biotin Blocking Kit (Vector Laboratories, Burlingame, CA). Sections were subsequently incubated with the primary antibodies at 4°C overnight. Next, sections were subjected to 3% $H_2O_2$ at room temperature for 10 minutes, followed by incubation with the secondary antibody at room temperature for 30 minutes. The immune reaction was performed with the Vectastain Elite ABC Kit (Vector Laboratories) and developed using DAB (Vector Laboratories) as substrate.

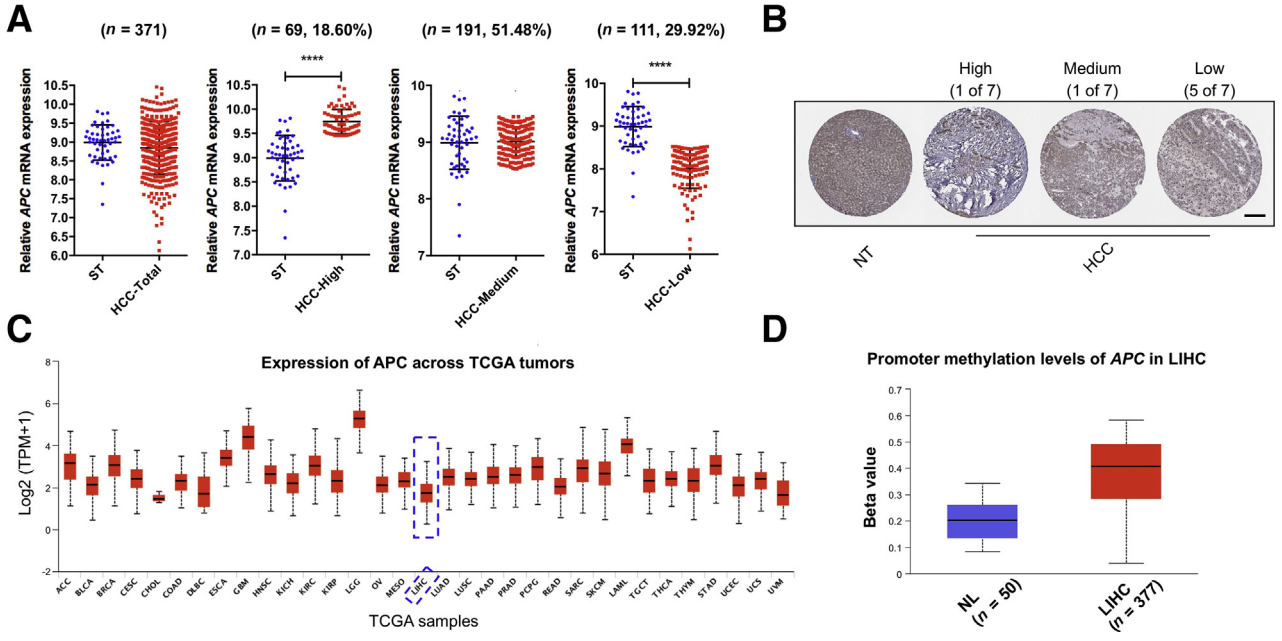


**Figure 2** APC expression status in human HCC samples. **A:** In comparison with the APC expression in surrounding tumor normal liver samples (mean ± SD = 8.989 ± 0.4675), HCC was classified into three subgroups (HCC-High, HCC-Medium, and HCC-Low) according to the APC expression. **B:** Immunohistochemistry images of APC in human HCC and normal liver tissues downloaded from the Human Protein Atlas website (*https://www.proteinatlas.org*, last accessed December 25, 2020). **C:** Extraction data from the UALCAN database (UALCAN, *http://ualcan.path.uab.edu*, last accessed December 25, 2020) to analyze APC expression patterns across human cancers. **Dashed boxes** indicate the expression of APC in liver hepatocellular carcinoma. **D:** Analysis of *APC* promoter methylation level in human HCC samples compared to normal liver samples based on the TCGA LIHC dataset. **B**–**D:** Images were downloaded from the Human Protein Atlas website and UALCAN website. Data were analyzed by *U*-test. $n = 50$ normal liver samples (**A**). ****$P < 0.0001$. Scale bar = 200 μm. ST, surrounding nontumorous liver tissue; HCC, hepatocellular carcinoma; NT, nontumorous liver; TCGA, The Cancer Genome Atlas; LIHC, liver hepatocellular carcinoma; NL, normal liver.

Subsequently, sections were counterstained with hematoxylin and covered-slipped with ClearMount mounting medium (StatLab, Lodi, CA). Detailed information on the antibodies for IHC is provided in Table 1.

### Protein Extraction and Western Blotting

Mouse liver tissues were homogenized for about 20 to 30 seconds and then lysed in M-PER Mammalian Protein Extraction Reagent (Thermo Fisher Scientific) containing the Halt Protease and Phosphatase Inhibitor Cocktail (Thermo Fisher Scientific). Extracted protein concentrations were quantified using the Pierce BCA Protein Assay Kit (Thermo Fisher Scientific) and then denatured in sample buffer (Laemmli Sample buffer: β-ME = 19:1) at 95°C for 5 minutes. For Western blotting, protein samples were separated by SDS-PAGE gel and transferred onto nitrocellulose membranes (Bio-Rad Laboratories, Hercules, CA). The membranes were blocked with 5% nonfat dry milk in Tris-buffered saline containing 0.1% Tween 20 at room temperature for 1 hour and then incubated with primary antibodies at 4°C overnight. Next, the membranes were incubated with horseradish peroxidase–conjugated secondary antibody (Jackson ImmunoResearch Laboratories, West Grove, PA) diluted 1:5000 at room temperature for 1 hour. After washing, membranes were developed using the SuperSignal West Pico PLUS Chemiluminescent Substrate (Thermo Fisher Scientific), and the blotting images were obtained by using the G-Box Gel Imaging System (Syngene USA, Frederick, MD). Detailed information on the antibodies for Western blot analysis is provided in Table 2.

### Quantitative Real-Time RT-PCR

Total RNA was extracted from mouse liver tissues using the Quick RNA Miniprep Kit (Zymo Research, Irvine, CA) and then converted to cDNA using the iScript Reverse Transcription Supermix (Bio-Rad Laboratories) following the manufacturer's protocol. Quantitative real-time RT-PCR (qRT-PCR) reactions were performed with 2.5 μL of cDNA (100 ng), 0.5 μL of forward primer, 0.5 μL of reverse primer, 5 μL of TaqMan Universal PCR Master Mix (Thermo Fisher Scientific), and 2.1 μL of distilled and deionized water. All qRT-PCR primers were purchased from Integrated DNA Technologies (Coralville, IA). qRT-PCR amplification cycles were performed on the QuantStudio6 Flex system (Applied Biosystems, Waltham, MA). Cycling conditions were as follows: polymerase activation at 95°C for 10 minutes, 40 cycles: denaturation at 95°C for 15 seconds, and extension at 60°C for 1 minute. Primer sequences are listed in Table 3.

### Statistical Analysis

All data are presented as means ± SD and analyzed with Prism version 6.0 software (GraphPad Software, San Diego, CA). Statistical analysis was performed using the *U*-test for nonparametric data or unpaired *t*-test for parametric data. The log-rank (Mantel-Cox) test was applied to analyze mice survival curves. $P < 0.05$ was considered statistically significant.

## Results

### *APC* Mutations and Expression Status in Human HCC and HB Samples

Although the Wnt signaling pathway plays a well-established pivotal role in liver tumorigenesis, little is known about the specific contribution of APC, a key regulator of the Wnt pathway, on liver oncogenesis. To characterize the molecular functions of APC in liver tumors,

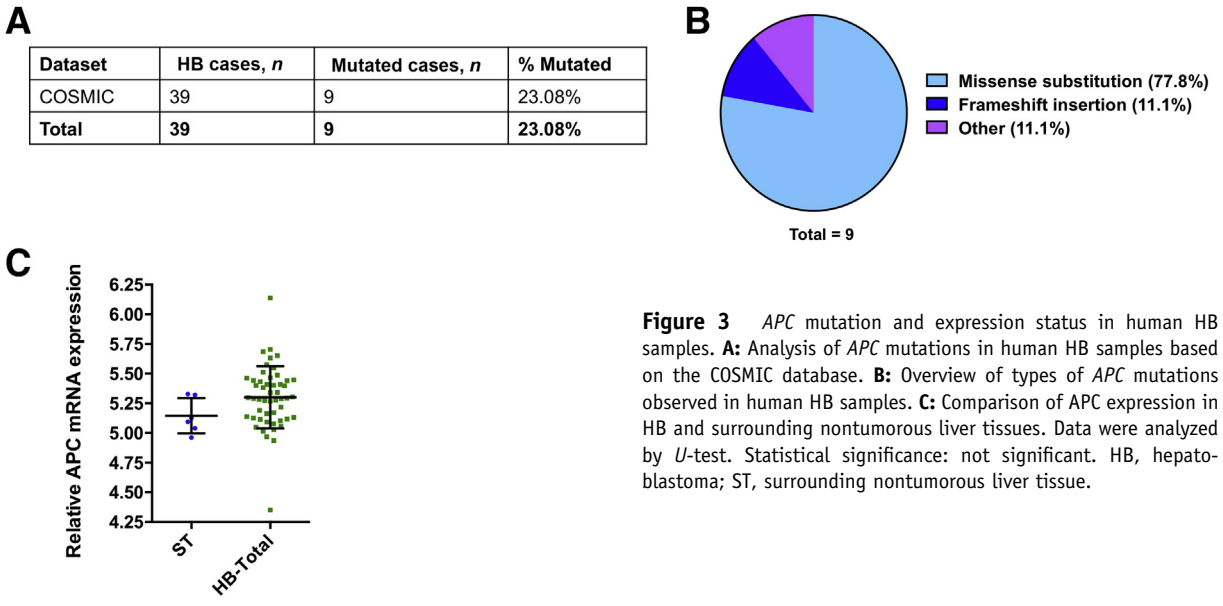


**Figure 3** *APC* mutation and expression status in human HB samples. **A:** Analysis of *APC* mutations in human HB samples based on the COSMIC database. **B:** Overview of types of *APC* mutations observed in human HB samples. **C:** Comparison of APC expression in HB and surrounding nontumorous liver tissues. Data were analyzed by *U*-test. Statistical significance: not significant. HB, hepatoblastoma; ST, surrounding nontumorous liver tissue.

the *APC* genomic alterations were first analyzed in human HCCs. cBioPortal for Cancer Genomics platform (cBioPortal, *https://www.cbioportal.org*, last accessed December 25, 2020) and the COSMIC database (COSMIC, *https://cancer.sanger.ac.uk/cosmic*, last accessed December 25, 2020), indicate that *APC* mutations occur in approximately 1.2% to 5.5% of HCC samples (Figure 1A). Among the mutations, 84.2% were LOF mutations, including nonsense substitutions, missense substitutions, truncating mutations, deep deletions, and frameshift insertions. These mutations accounted for 10.5%, 49.5%, 19.3%, 3.5% and 1.8%, of all *APC* mutations, respectively (Figure 1B). *APC*-inactivating mutations identified in HCCs are consistent with the hypothesis that APC functions as a tumor suppressor in HCC.

Next, the APC mRNA levels in human HCC samples were evaluated. A total of 371 HCC tissues and 50 normal liver tissues from The Cancer Genome Atlas Liver Hepatocellular Carcinoma (TCGA LIHC) dataset were used for analysis.[43] APC mRNA expression varied significantly among HCC samples (Figure 2A). Subsequently, HCCs were subdivided into three subgroups according to the APC expression level compared with non-tumor liver tissues. The results suggest that approximately 20% of HCCs have higher APC expression; approximately 50% have similar expression; and approximately 30% show lower APC expression when compared with corresponding non-neoplastic surrounding liver tissue (Figure 2A). The decreased APC mRNA expression detected in a subset of HCCs was also consistent with APC protein expression pattern in HCC patients. Five of seven HCC patients revealed a lower APC protein level compared with normal liver tissues based on the Human Protein Atlas dataset (Human Protein Atlas, *https://www.proteinatlas.org*, last accessed December 25, 2020) (Figure 2B). It is worth noting that in comparison with other human cancers, APC is expressed at a very low level in HCC (Figure 2C).

Since *APC* promoter methylation has been reported in cancer, including in HCC,[44] *APC* promoter methylation status in human HCC was investigated. APC promoter hypermethylation occurred in 78% of human HCC patients.[45] Based on the UALCAN analysis (UALCAN, *http://ualcan.path.uab.edu/index.html*, last accessed December 25, 2020), a significantly increased *APC* promoter methylation was observed in HCC compared with normal liver (Figure 2D). No correlation was found

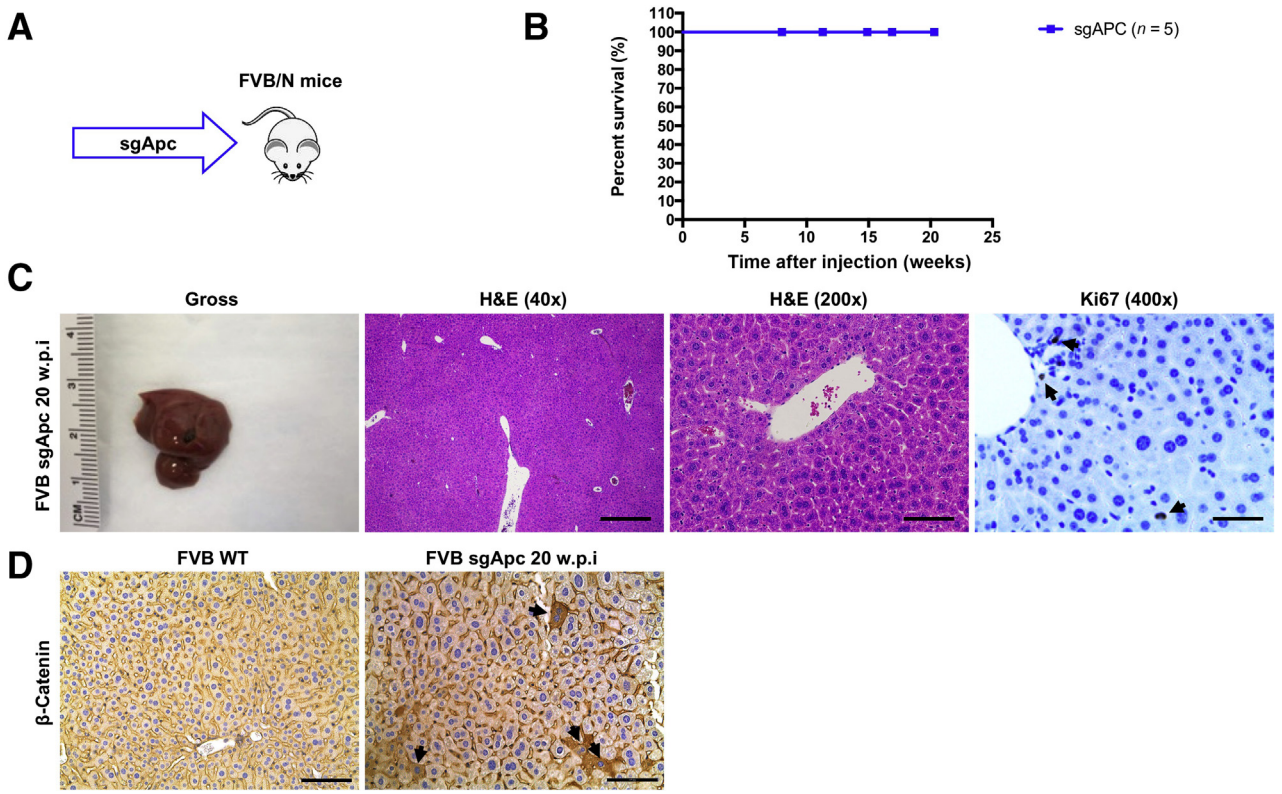


**Figure 4** Deletion of Apc alone fails to induce liver tumor formation in mice. **A:** Study design. FVB/N male mice were injected with the sgApc plasmid. **B:** Mouse survival curves. **C:** Representative gross images, H&E, and immunohistochemistry for proliferation cell marker Ki-67 of liver sections from the sgApc mice. Note that the liver of sgApc mice appears completely normal and displays only a few Ki-67–positive cells (**arrows**). **D:** Immunohistochemical staining of β-catenin. Few β-catenin–positive cells (**arrows**) are visible in the liver parenchyma of the sgApc mouse. $n = 5$ mice (**A**). Scale bars: 500 μm (**C**, **left H&E panel**); 100 μm (**C**, **right H&E panel**); 50 μm (**C**, **Ki67 panel**). Original magnification: ×40 (**C**, **left H&E panel**); ×200 (**C**, **right H&E panel**, and **D**); ×400 (**C**, **Ki67 panel**). H&E, hematoxylin and eosin; w.p.i, weeks post-injection; WT, wild type.

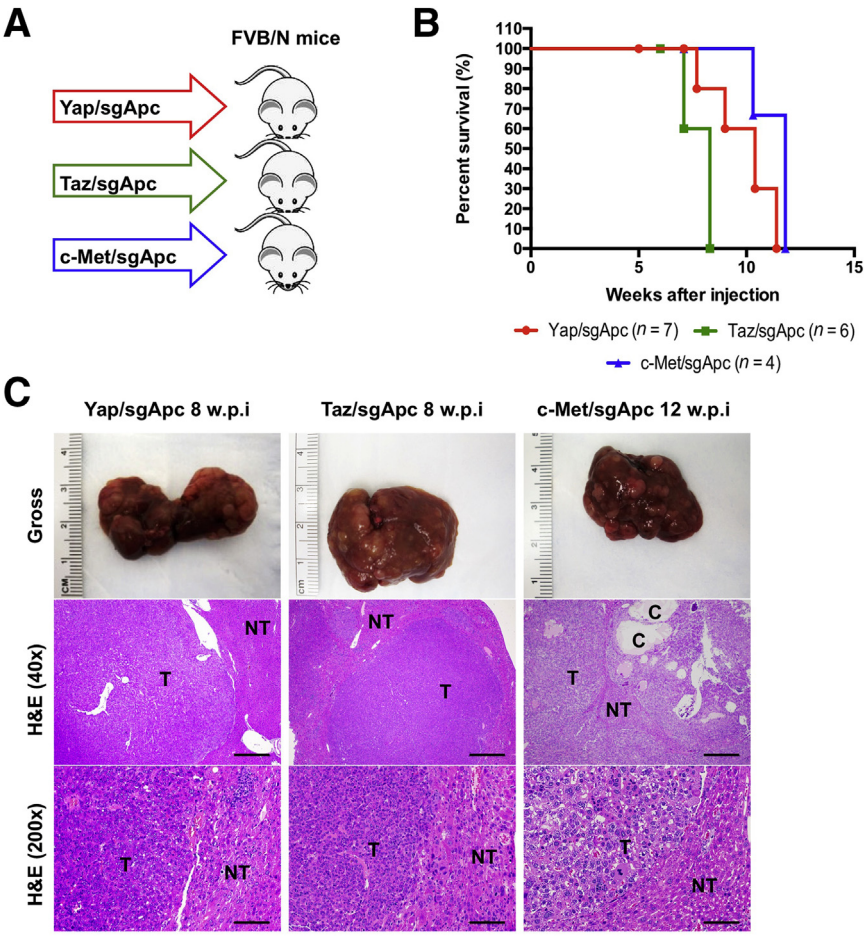


**Figure 5** Deletion of Apc cooperates with YapS127A to induce liver tumor formation in mice. **A:** Study design. FVB/N male mice were injected with Yap/sgApc, Taz/sgApc or c-Met/sgApc plasmids, respectively. **B:** Mouse survival curves. **C:** Representative gross images and H&E of liver sections from Yap/sgApc, Taz/sgApc, and c-Met/sgApc mice. Tumors developing in Yap/sgApc and Taz/sgApc mice were virtually identical and consisted of small cells with prominent nuclei forming solid lesions that resemble human fetal hepatoblastoma. At ×200 magnification, the smaller size of tumor cells when compared with nontumorous surrounding hepatocytes can be better appreciated. By contrast, tumor lesions developing in c-Met/sgApc mice resembled more closely human HCC and were composed of bigger cells with a larger cytoplasm, frequently with a clear cell phenotype (better appreciable at higher magnification). In particular, c-Met/sgApc tumor cells grew in solid and trabecular patterns, and cysts were often observed within the tumors. The image at higher magnification shows the similar size of surrounding normal hepatocytes and c-Met/sgApc tumor cells. $n = 7$ mice with Yap/sgApc plasmids (**A**); $n = 6$ mice with Taz/sgApc plasmids (**A**); $n = 4$ mice with c-Met/sgApc plasmids (**A**). Scale bars: 500 μm (**C, middle row**); 100 μm (**C, bottom row**). C, cysts; H&E, hematoxylin and eosin; NT, nontumorous liver; T, tumors; w.p.i, weeks post-injection.

between *APC* promoter methylation and APC mRNA expression using the MEXPRESS tool[46] (MEXPRESS, *https://mexpress.be/index.html*, last accessed December 25, 2020), (Supplemental Figure S1). The results indicate that promoter methylation is not a major mechanism regulating APC mRNA expression in human HCCs.

Finally, whether APC demonstrates similar genomic alterations and expression patterns in human HBs was analyzed. Based on the COSMIC database, *APC* was mutated in 23.08% of HB specimens (Figure 3A). Among them, 77.8% of the mutations were missense substitutions, whereas the remaining 11.1% were frameshift insertions (Figure 3B). The APC mRNA expression pattern was retrieved from the microarray study by Sumazin et al,[47] which showed no significant difference between HB and normal liver (Figure 3C). However, it is important to underline that the sample size was very small, and the results need to be further validated.

Altogether, LOF *APC* mutations were identified in approximately 3% of human HCC and approximately 23% of human HB samples. In addition, down-regulation of *APC* was found in 30% of HCC samples. Overall, these data suggest a potential tumor suppressor role of APC during hepatocarcinogenesis.

## Deletion of Apc Activates β-Catenin, but Does Not Promote Liver Tumor Formation in Mice

To further investigate the tumor suppressor function of APC during liver tumor development, the effect of deletion of Apc on induction of liver tumor formation in mice was evaluated. The CRISPR-Cas9–based gene deletion (sgApc) and hydrodynamic injection methods were applied to delete Apc in a subset of mouse hepatocytes (Figure 4A). The study design was similar to that described in our previous paper in which Axin1 was deleted in the mouse liver.[48] Deletion of Apc via hydrodynamic injection of the sgApc plasmid did not lead to liver tumor formation. Mice were completely healthy even at 20 weeks post-injection (Figure 4, B and C). Grossly, the liver appeared to be normal with no visible surface nodules (Figure 4C). Histologic evaluation also revealed the absence of alterations in the sgApc liver parenchyma, with few Ki-67–positive proliferating cells (Figure 4C). Only membranous β-catenin staining was detected in the uninjected normal liver by IHC. By contrast, cytoplasmic/nuclear β-catenin staining in sporadic hepatocytes was observed in sgApc-injected mouse liver tissues, indicating that the loss of Apc leads to the activation of β-catenin in these hepatocytes (Figure 4D).

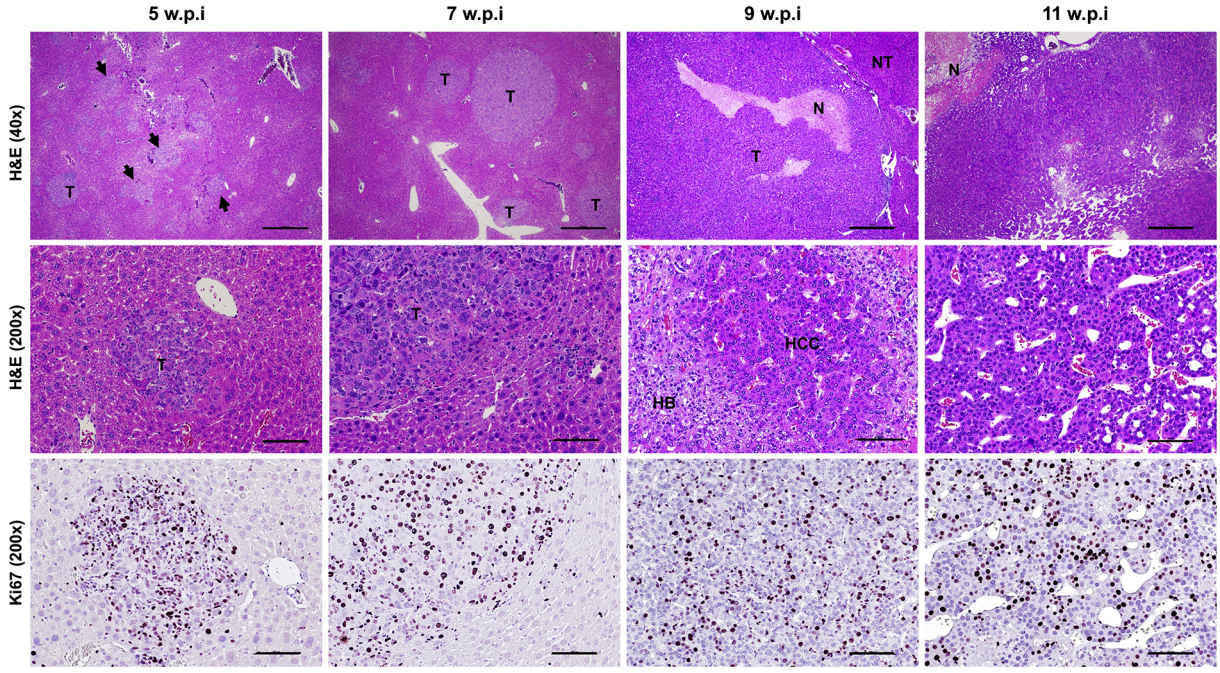


**Figure 6** Stepwise development of liver tumor lesions in Yap/sgApc mice. Focal preneoplastic lesions (**arrowheads**) and small tumors emerging in the liver parenchyma of Yap/sgApc as early as 5 weeks post-injection are shown in the **left column** in two magnifications. Tumors and focal lesions were characterized by small cells with a prominent nucleus growing in a solid pattern (note the small size of tumor cells when compared with surrounding nontumorous cells in the high magnification image) and were actively proliferating, as assessed by Ki-67 staining. By 7 weeks post-injection, most of the preneoplastic lesions were replaced by small and larger tumors retaining the histomorphologic features of the earlier lesions. At 9 weeks post-injection, most of the liver surface was occupied by rapidly growing tumors, as assessed by the presence of areas of necrosis. Importantly, at this time, lesions composed of HCC-like cells (HCC) start to emerge in the liver parenchyma of Yap/sgApc mice. These cells, better appreciated at higher magnification, displayed a larger nucleus and cytoplasm of those from HB-like cells (HB) and grew mainly as a trabecular pattern. By 11 weeks post-injection, almost the whole liver was occupied by HCC-like lesions that have replaced the HB-like lesions. Scale bars: 500 μm (**top row**); 100 μm (**middle** and **bottom rows**). Original magnification: ×40 (**top row**); ×200 (**middle** and **bottom rows**). H&E, hematoxylin and eosin; N, necrosis; NT, nontumorous liver; T, tumors; w.p.i, weeks post-injection.

Overall, approximately 2% of hepatocytes in the mouse liver exhibited loss of Apc-induced cytoplasmic/nuclear β-catenin staining.

Altogether, the data show that deletion of Apc in a subset of mouse hepatocytes activates β-catenin, but it is unable to promote liver tumor development *in vivo*.

## Deletion of Apc Cooperates with YapS127A, TazS89A, or c-Met Oncogenes to Induce Liver Tumor Formation in Mice

Activation of YAP, TAZ, and c-MET are common oncogenic events in human HCCs.[29,30,49,50] Using the c-MET activation gene expression signature,[48] approximately 18% of human HCC samples were estimated to have low APC expression and c-MET activation. In addition, in a recent investigation, we showed that almost all human HCC samples have nuclear/activated YAP and/or TAZ.[51] Therefore, most of the HCC samples with low APC expression likely have either YAP and/or TAZ activation. Activated *CTNNB1* mutations, such as ΔN90-β-catenin, cooperate with activated forms of Yap (YapS127A), Taz (TazS89A), or overexpression of c-Met to promote liver tumor development.[37,40,52] Here, we hypothesized that loss of Apc may similarly synergize with these activated oncogenes to promote liver tumor formation. To validate this hypothesis, mice were subjected to hydrodynamic injection of sgApc together with either YapS127A (Yap/sgApc), TazS89A (Taz/sgApc), or c-Met (c-Met/sgApc), and monitored for liver tumor development (Figure 5A). Yap/sgApc, Taz/sgApc, and c-Met/sgApc mice uniformly developed high liver tumor burden and were moribund between 8 and 12 weeks after injection (Figure 5B). Microscopically, tumors were characterized by small, round cells resembling human HB in Yap/sgApc and Taz/sgApc mice. By contrast, c-Met/sgApc mouse tumors were composed of larger HCC-like cells, growing in a solid or trabecular pattern and frequently forming cystic lesions (Figure 5C). The overexpression of exogenous oncogenes, as well as the loss of Apc expression, was confirmed using Western blotting and IHC in Yap/sgApc, Taz/sgApc, and c-Met/sgApc models (Supplemental Figures S2 and S3).

In the Yap/sgApc mice, liver tumors could be detected as early as approximately 5 weeks post-injection (Figure 6). As reported above, tumors consisted of minute cells with prominent nuclei, similar to those previously described in Yap/β-catenin mice[52] (Supplemental Figure S4), and resembling human fetal or crowded fetal HB. The HB-like

lesions progressively expanded and occupied about 30% to 40% of the liver parenchyma by 7 to 9 weeks post-injection, and by 10 to 11 weeks post-injection, the vast majority of the liver surface was replaced by colliding tumors. Of note, a second, distinct tumor entity was appreciable in the liver parenchyma of Yap/sgApc mice starting by 9 weeks post-injection. At this time, the HB-like cells coexisted with larger HCC-like cells, organized in trabeculae, and exhibited a bigger nucleus and a prominent, highly basophilic cytoplasm. The HCC-like cells (and related HCC-like lesions) almost completely replaced the HB-like lesions in Yap/sgApc mice by 11 weeks post-injection (Figure 6). Because the primary role of APC is to impair β-catenin activation in the cell, it can be envisaged that Apc loss would phenocopy the effect of β-catenin activation in the liver. Thus, the Yap/sgApc mouse liver lesions were compared with those developed by Yap/β-catenin mice. Yap/sgApc and Yap/β-catenin mice showed similar overall survival and tumor burden (Supplemental Figure S4, A and B). Consistently, positive Ki-67 staining in tumor tissues from Yap/sgApc mice showed no significant difference when compared with that from Yap/β-catenin mice (Supplemental Figure S4C). However, the development of HCC-like lesions was limited to Yap/sgApc mice. Importantly, the replacement of HB-like lesions by HCC-like lesions was also detected in Taz/sgApc mice (Supplemental Figure S5).

Similar results in terms of proliferation, overall survival, and tumor burden were also observed in Taz/sgApc and c-Met/sgApc mouse lesions when compared with those from Taz/β-catenin and c-Met/β-catenin mice, respectively, from our previous reports (Supplemental Figure S6).[37,53]

Collectively, these results demonstrate that loss of Apc cooperates with activated oncogenes, including Yap, Taz, and c-Met to promote liver tumor formation in mice.

## Molecular Characterization of Liver Lesions from Yap/sgApc, Taz/sgApc, and c-Met/sgApc Mice

Molecular features of the lesions developed in the three newly generated mouse models were investigated by IHC in both early and late tumor lesions developed in Yap/sgApc, Taz/sgApc, and c-Met/sgApc mice. In the early lesions (Figure 7), Yap/sgApc, Taz/sgApc, and c-Met/sgApc mice displayed heterogeneous nuclear, cytoplasmic, and membranous staining for β-catenin, with fewer nuclear-positive cells and mostly membranous staining detected in c-Met/sgApc mice. Levels of the β-catenin–specific target glutamine synthetase (GLUL) were strongly induced in the early tumor lesions of the three mouse models, with no overt differences related to the genes injected (Supplemental Figure S7). Analysis of the levels of canonical markers of mature hepatocytes indicated that the nuclear staining intensity for hepatocyte nuclear factor 4-alpha (HNF4α) and CCAAT enhancer-binding protein alpha (CEBPα) was lower in the lesions when compared with that in the surrounding nontumorous liver in Yap/sgApc and Taz/sgApc mice. By contrast, levels of HNF4α and CEBPAα were equivalent in tumor lesions and surrounding liver tissues in c-Met/sgApc mice (Figure 7). On the other hand, immunoreactivity for the progenitor marker SRY-box transcription factor 9 (SOX9) and the cholangiocyte markers cytokeratin 7 (CK7) and 19 (CK19) was pronounced in Yap/sgApc and Taz/sgApc early lesions, whereas

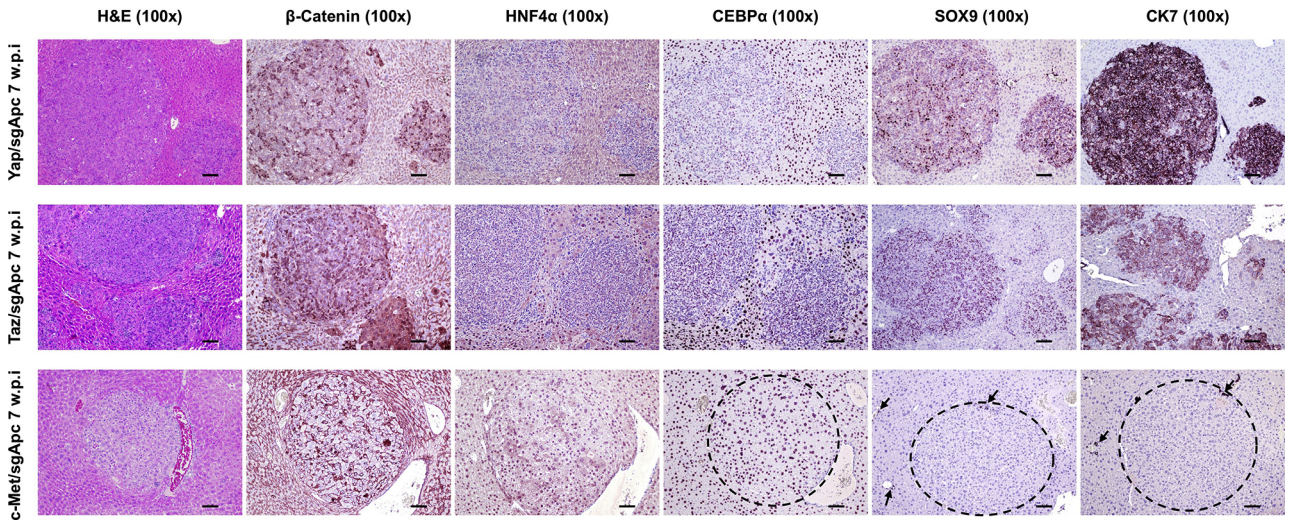


**Figure 7** Molecular characterization of early liver lesions developed in Yap/sgApc, Taz/sgApc, and c-Met/sgApc mice by immunohistochemistry. Staining patterns for β-catenin as well as for hepatocellular (HNF4α, CEBPα), progenitor (SOX9), and cholangiocellular (CK7) markers are shown in each image. Preneoplastic lesions (not shown) and HB-like tumors from Yap/sgApc and Taz/sgApc mice exhibited lower nuclear levels of HNF4α and CEBPα hepatocellular markers when compared with the adjacent nontumorous surrounding liver, whereas corresponding lesions from c-Met/sgApc mice displayed similar levels of the same proteins in the tumorous and nontumorous compartments. **Dashed circles** indicate c-Met/sgApc lesions. Levels of the SOX9 progenitor marker as well as of the CK7 cholangiocellular marker were elevated in Yap/sgApc and Taz/sgApc lesions, and immunoreactivity for SOX9 and CK7 was limited to normal biliary cells (**arrows**) in c-Met/sgApc livers. Scale bars = 100 μm. Original magnification, ×100.

immunolabeling for the same proteins was limited to normal biliary cells in c-Met/sgApc livers (Figure 7 and Supplemental Figure S7). Immunohistochemical pattern for members of the *de novo* lipogenic pathway, a pivotal signaling cascade in human HCC, as well as in c-Met–driven hepatocarcinogenesis were analyzed.[29,54] A weaker expression of both fatty acid synthase (FASN) and stearoyl-CoA desaturase 1 (SCD1) was found in the early liver lesions when compared with surrounding nontumorous liver tissue of Yap/sgApc and Taz/sgApc mice, whereas a strong immunoreactivity for the two proteins emerged in the tumor lesions from c-Met/sgApc mice (Supplemental Figure S7).

Because the histopathologic features of Yap/sgApc and Taz/sgApc lesions indicated a differentiation toward HCC lesions at a late stage of tumorigenesis, whether the observed histologic changes were accompanied by modifications in staining patterns of the same proteins investigated in early lesions was investigated (Figure 8). Interestingly, Yap/sgApc and Taz/sgApc advanced lesions exhibited cytoplasmic and membranous immunoreactivity for β-catenin protein, as determined by IHC, whereas nuclear localization of β-catenin was retained in the corresponding lesions developed in c-Met/sgApc mice (Figure 8). Equivalent, high levels of GLUL were observed in the lesions of the three mouse models (Supplemental Figure S8). In terms of mature hepatocyte markers, nuclear immunoreactivity for HNF4α and CEBPα was similar in the lesions of the three mouse cohorts, with staining intensity equivalent to that of the corresponding surrounding nontumorous liver tissue. Immunoreactivity for CK7 and CK19 proteins was retained in HCC-like lesions from Yap/sgApc and Taz/sgApc mice and absent in c-Met/sgApc lesions (Figure 8 and Supplemental Figure S8). Of note, immunoreactivity for SOX9 was almost completely lost in Yap/sgApc and Taz/sgApc HCC-like lesions when compared with early lesions of the same mice. No positive staining for SOX9 was detected in corresponding lesions from c-Met/sgApc mice. Moreover, an equally high expression of FASN and SCD1 proteins was detected in the advanced lesions of the three mouse models (Supplemental Figure S8).

Overall, these data indicate that tumors developing in Apc-deleted livers display different features depending on the injected oncogene associated with specific molecular features. In particular, HB-like liver lesions from Yap/sgApc and Taz/sgApc mice were characterized by low levels of mature hepatocyte and lipogenesis markers, which underwent up-regulation in the advanced tumors.

## Loss of Apc and Activation of β-Catenin Drive the Induction of Common and Distinct Targets in Mouse Tumors

Molecular features of mouse tumors depleted of Apc were compared with those harboring activated β-catenin. Given that loss of APC stabilizes and activates β-catenin,[55] whether β-catenin and its downstream target GLUL, were similarly activated in Yap/sgApc, Taz/sgApc, and c-Met/sgApc mouse tumors and in corresponding liver lesions from Yap/β-catenin, Taz/β-catenin, and c-Met/β-catenin mice was investigated (Supplemental Figures S9 and S10).[37,40,52] Strong nuclear β-catenin staining was detected in both Yap/sgApc- and Yap/β-catenin–induced liver tumors (Supplemental Figure S9, A and B). Intriguingly, consistent with our previous report,[52] the immunohistochemical pattern for GLUL was highly heterogeneous in Yap/β-catenin malignant lesions, with some nodules positive and others negative for

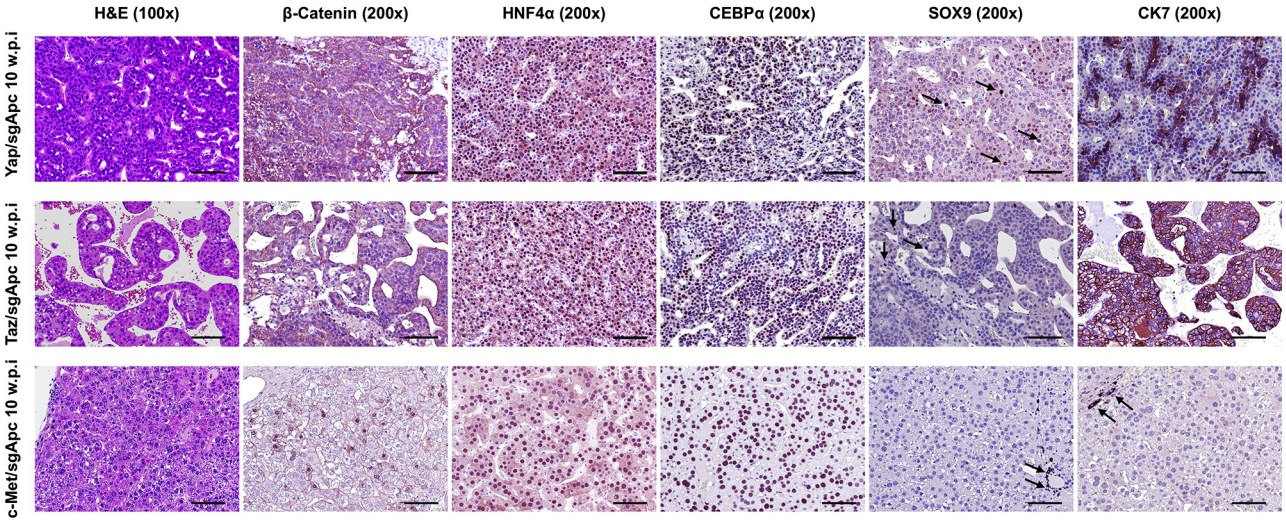


**Figure 8** Molecular features of advanced liver lesions developed in Yap/sgApc, Taz/sgApc, and c-Met/sgApc mice by immunohistochemistry. Staining patterns for β-catenin, as well as for hepatocellular (HNF4α, CEBPα), progenitor (SOX9), and cholangiocellular (CK7) markers, are shown in each image. Positive immunolabeling for SOX9 (**arrows**, **top** and **middle rows**) and normal biliary cells. CK7 staining in biliary epithelial cells (**arrows, bottom row**) of c-Met/sgApc livers. Scale bars = 100 μm. Original magnification: ×100 (**left column**); ×200 (**all other columns**).

staining (Supplemental Figure S9, C and D). By contrast, all Yap/sgApc-corresponding lesions demonstrated uniform positive immunoreactivity for GLUL staining (Supplemental Figure S9, C and D). Similar results were observed in the other two mouse models. Specifically, β-catenin and GLUL were concomitantly and diffusely activated in liver tumors from Taz/sgApc and c-Met/sgApc mice, whereas GLUL up-regulation was not uniform in Taz/β-catenin and c-Met/β-catenin mouse lesions (Supplemental Figure S10). These results highlight the difference of GLUL expression patterns in liver tumors induced by LOF *APC* and GOF *Ctnnb1* mutations. Glutamine directly phosphorylates mTOR at Ser2448 in lysosomes,[56] and increased GLUL leads to augmented p-mTOR-Ser2448 in the liver.[57] Therefore, p-mTOR-Ser2448 levels in the mouse liver tumor samples were investigated. Liver tumors in Yap/sgApc, Taz/sgApc, and c-Met/sgApc models were positive for p-mTOR-Ser2448, as determined by IHC (Supplemental Figures S11–S13). By contrast, some tumor lesions in Yap/β-catenin, Taz/β-catenin, and c-Met/β-catenin models were GLUL-negative, and also stained negative for p-mTOR-Ser2448 (Supplemental Figures S11–S13). Based on the present findings, it can be concluded that LOF *APC* mutations, but not GOF *Ctnnb1* mutations, consistently induce GLUL and p-mTOR-Ser2448 expression during liver tumor development.

Subsequently, additional molecular markers were compared in mice harboring either the loss of Apc or the activation of mutant β-catenin. For this analysis, Yap/sgApc-induced liver tumors in the Yap/sgApc mice were compared with corresponding Yap/β-catenin lesions (Figure 9). First, the overexpression of Yap, as well as the loss of Apc expression, was confirmed with Western blotting (Figure 9A). Next, qRT-PCR analysis was performed to analyze the genes downstream of Wnt/β-catenin and Yap pathways in the liver tumor samples. A subset of Wnt target genes, including *Myc*, *Ccnd1*, *Axin2*, *Lgr5*, and *Lect2*, were up-regulated and expressed at similar levels in both Yap/sgApc and Yap/β-catenin liver tumors (Figure 9B), whereas other targets, including *Glul*, *Tbx3*, and *Sp5*, were up-regulated in tumor samples, but exhibited higher expression levels in Yap/sgApc tumors than in Yap/β-catenin lesions (Figure 9B). Yap target genes, including *Ccn2* (*Ctgf*), *Ccn1*(*Cyr61*), and *Jag1*, were up-regulated in liver tumor samples at similar levels (Figure 9B). Additional members of the Notch signaling, such as *Notch2*, *Hes1*, and *Hey1*, were more elevated in Yap/sgApc lesions. Furthermore, hepatic tumor markers, including *Afp*, *Gpc3*, and *Epcam*, were significantly increased in Yap/sgApc and Yap/β-catenin liver tumors compared with the normal liver tissues (Figure 9B).

In summary, this analysis suggests that both LOF *APC* mutations and GOF *Ctnnb1* mutations trigger the activation of the Wnt/β-catenin pathway. However, LOF *APC* mutations, but not GOF *Ctnnb1* mutations, demonstrate uniform activation of GLUL and p-mTOR in liver tumors.

## Yap/sgApc Activation Triggers Liver Tumor Development via the β-Catenin/TCF4 Pathway

Because the *in vivo* data indicated that loss of Apc induces Wnt/β-catenin activation in mouse HCC, whether Wnt/β-

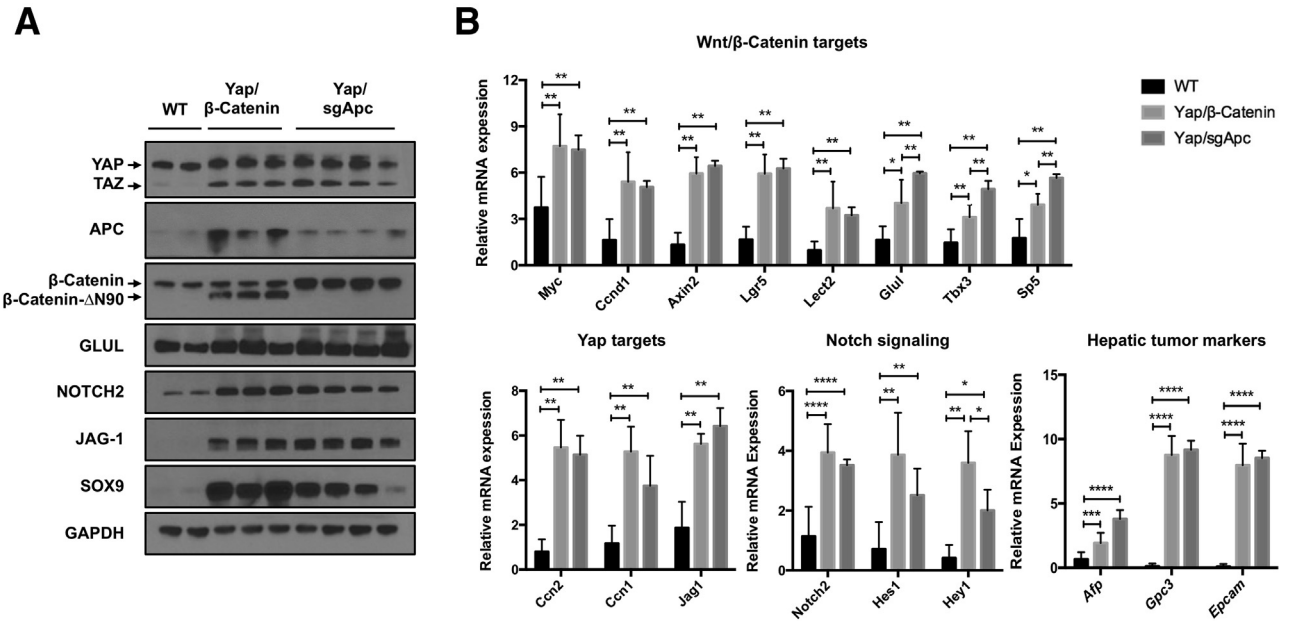


**Figure 9** Molecular features of Yap/β-catenin and Yap/sgApc mouse tumors. **A:** Western blot analysis of Wnt/β-catenin and Hippo/Yap signaling pathways in wild-type livers (WT), and Yap/β-catenin and Yap/sgApc tumor lesions. GAPDH was used as a loading control. **B:** Quantitative real-time RT-PCR (qRT-PCR) analysis of Wnt/β-catenin, Hippo/Yap, and Notch pathway genes, and hepatic tumor markers expression in liver tissues from the indicated mice. rRNA mRNA expression was used as the internal control. Data were analyzed by *U*-test. $*P < 0.05$, $**P < 0.01$, $***P < 0.001$, and $****P < 0.0001$. WT, wild type.

catenin is required for LOF *APC* mutation-driven hepatocarcinogenesis was investigated in the Yap/sgApc mouse model and *Ctnnb1*$^{f/f}$ conditional knockout (KO) mice[48]. In brief, Yap and sgApc plasmids together with pCVM/Cre vector were hydrodynamically injected into *Ctnnb1*$^{f/f}$ mice. This allowed the expression of Yap/sgApc oncogenes in *Ctnnb1* KO hepatocytes (Figure 10A). Additional *Ctnnb1*$^{f/f}$ mice were injected with Yap and sgApc together with pCMV empty vector as control (Figure 10A). Similar to that described previously (Figure 5), Yap/sgApc/pCMV-injected *Ctnnb1*$^{f/f}$ mice developed liver tumors, became moribund, and had to be euthanized by 12 weeks post-injection (Figure 10B). By contrast, Cre-dependent ablation of the endogenous β-catenin completely inhibited Yap/sgApc-induced liver tumor development in mice. All Yap/sgApc/Cre-injected *Ctnnb1*$^{f/f}$ mice appeared to be healthy with no palpable abdominal mass even at 20 weeks post-injection (Figure 10B). Upon dissection, the total liver weight of Yap/sgApc/Cre mice was similar to that of uninjected mice, whereas that of Yap/sgApc/pCMV mice was higher due to tumor burden (Figure 10C). Grossly, numerous tumor nodules were detected on the liver surface of Yap/sgApc/pCMV-injected *Ctnnb1*$^{f/f}$ mice, whereas no tumors were found in Yap/sgApc/Cre-injected mice (Figure 10D). Histologically, HB-like and HCC-like lesions occupied most of the liver parenchyma in Yap/sgApc/pCMV mice. By contrast, liver tissues from Yap/sgApc/Cre mice were completely normal and could not be distinguished from those of uninjected mice (Figure 10D). Altogether, these data demonstrate that endogenous β-catenin is required for Yap/sgApc-induced liver tumor development in mice.

It is well established that Wnt/β-catenin promotes tumor development via TCF4-mediated transcriptional activity.[58] To further investigate the molecular mechanisms whereby β-catenin controls hepatocarcinogenesis, the role of functional TCF4 in Yap/sgApc-induced liver tumor formation was investigated by using the dominant negative form of TCF4 (dnTCF4), which effectively inhibits β-catenin−dependent transcription.[59] Mice were hydrodynamically injected with Yap and sgApc plasmids together with pT3-EF1α-dnTCF4 (Yap/sgApc/dnTCF4) or pT3-EF1α empty vector (Yap/sgApc/pT3) as control (Figure 11A). Similar to that observed in conditional *Ctnnb1* KO mice, dnTCF4 completely blocked Yap/sgApc-induced HB-like and HCC-like lesions formation in mice (Figure 11, B−D). These data demonstrate that TCF4-mediated transcriptional regulation is strictly required for Yap/sgApc-driven hepatocarcinogenesis.

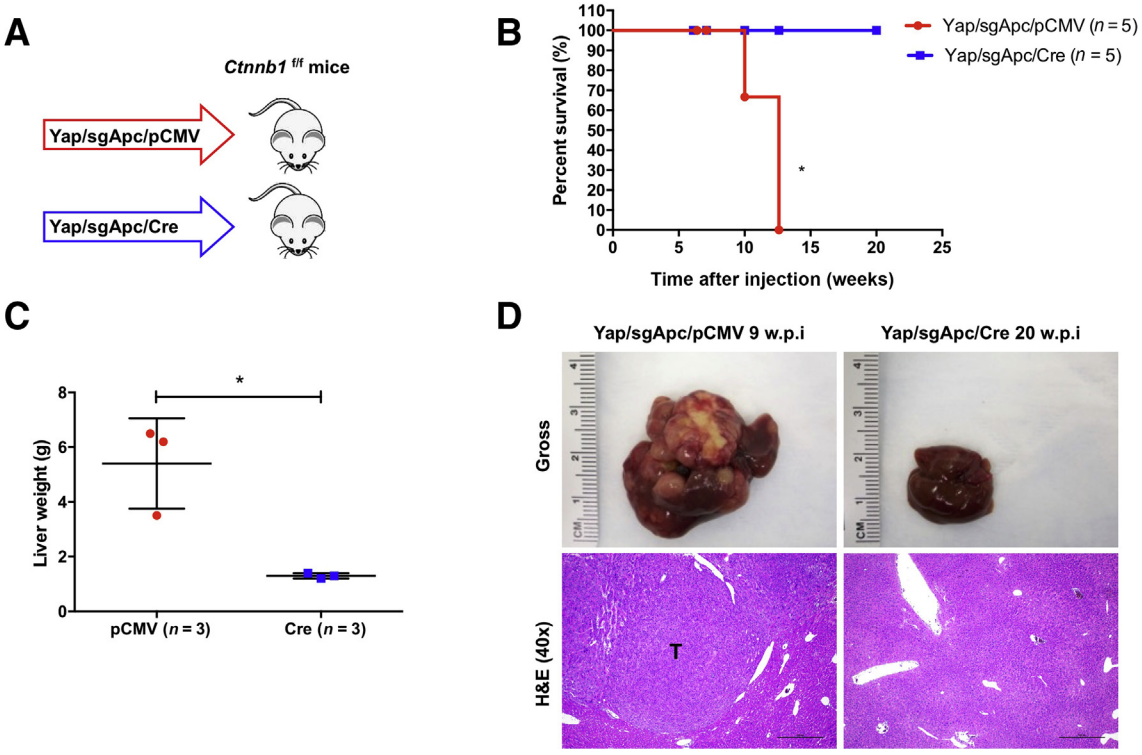


**Figure 10** Ablation of *Ctnnb1* completely inhibits YAP/sgApc-induced hepatocarcinogenesis. **A:** Study design. *Ctnnb1*$^{f/f}$ mice were injected with YAP/sgApc/pCMV or YAP/sgApc/Cre plasmid. **B:** Kaplan-Meier curves showing survival of the mice. The log-rank (Mantel-Cox) test was applied for the analysis of mice survival curves. **C:** Analysis of liver weight of the indicated *Ctnnb1*$^{f/f}$ mice at late stage (9.0 to 20.0 w.p.i). **D:** Representative gross images and H&E of mouse livers. Data are expressed as means ± SD (**C**). $n = 5$ mice with YAP/sgApc/pCMV plasmids (**A**); $n = 5$ mice with YAP/sgApc/Cre plasmids (**A**). *$P < 0.05$ (unpaired *t*-test). Scale bars = 500 μm. Original magnification, ×40. H&E, hematoxylin and eosin; T, tumors; w.p.i, weeks post-injection.

In summary, this study demonstrates that liver tumor development driven by the loss of Apc requires an intact β-catenin/TCF4 axis in mice.

### Tumor Progression Is Sex-Dependent in Yap/sgApc and Taz/sgApc Mice

Finally, to assess whether sex influences tumor development and progression induced by loss of Apc, the tumor development of Yap/sgApc, Taz/sgApc, and c-Met/sgApc was determined in male and female mice (Figure 12 and Supplemental Table S1). No difference in tumor incidence was observed, as all male and female mice from the three cohorts developed high tumor burden regardless of their sex. In addition, no difference in tumor histopathologic features was observed in male and female mice (not shown). Of note, a significantly longer survival was observed in female Yap/sgApc and Taz/sgApc mice when compared with male mice, especially in the Yap/sgApc model (Figures 12 and Supplemental Table S1). However, no difference in survival length was found in c-Met/sgApc male and female mice (Supplemental Table S1).

Altogether, these data indicate that tumor progression is influenced by sex in Yap/sgApc and Taz/sgApc mice.

## Discussion

*APC* is a classical tumor suppressor gene, and LOF *APC* mutations have been implicated in multiple tumor types, especially in colorectal cancer.[60] Studies on APC in liver cancer, including HCC and HB, are scanty. The present investigation provides a comprehensive analysis of *APC* mutation status and expression in human HCC and HB using public datasets. LOF *APC* mutations occurred in approximately 2.76% of HCCs and 23.08% of HBs, whereas down-regulation of APC mRNA was found in about 30% of HCCs. Overall, this body of data is consistent with the hypothesis that APC functions as a tumor suppressor during hepatocarcinogenesis.

In mice, ablation of Apc alone was unable to induce liver tumor formation. A previous study demonstrated that liver specific deletion of Apc results in HCC development around 8 to 9 months after gene ablation.[61] The reasons for these disparate findings are unkown. In the published study, Apc was deleted in all mouse hepatocytes, and tumor developed after a very long latency. It is possible that additional genetic events in the hepatocytes over time may have lead to HCC formation in the whole liver of *Apc* KO mice. By contrast, here, Apc was deleted only in sporadic hepatocytes using the combination of CRISPR-Cas9–based gene

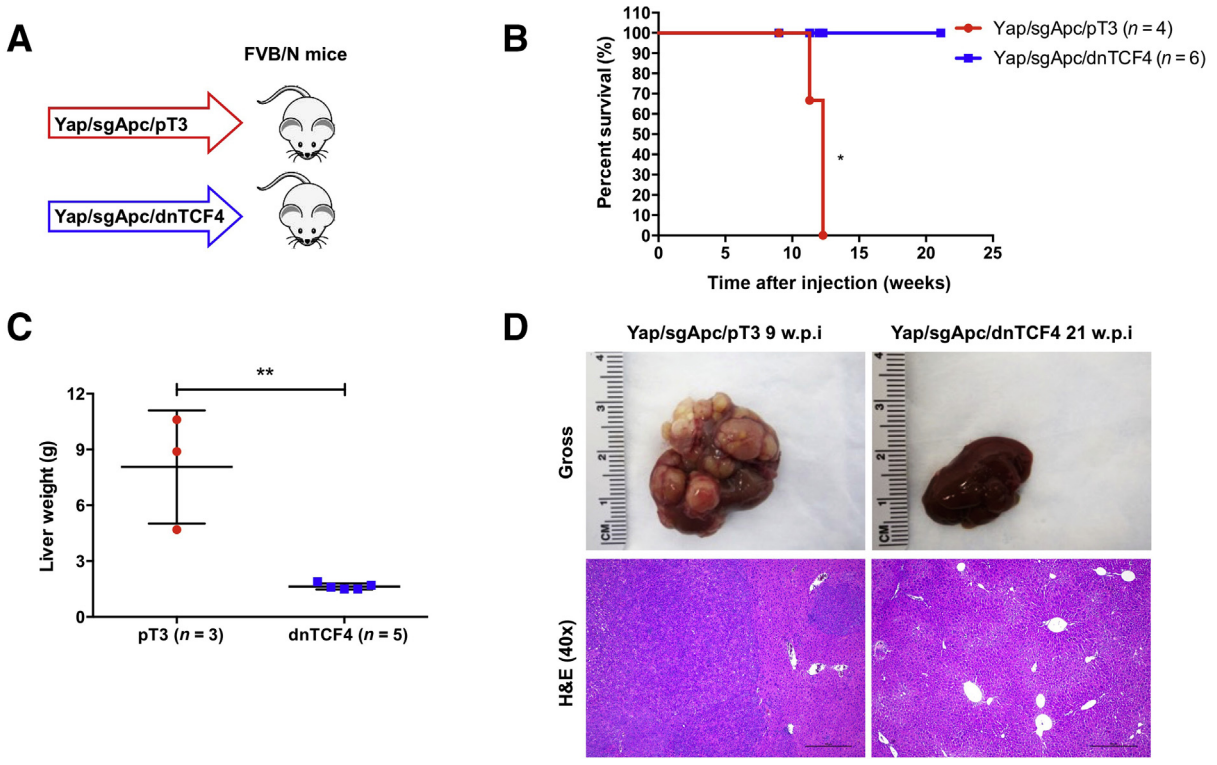


**Figure 11** TCF4 is required for Yap/sgApc-driven hepatocarcinogenesis in mice. **A:** Study design. FVB/N mice were injected with YAP/sgApc/pT3 or YAP/sgApc/dnTCF4 plasmid. **B:** Kaplan-Meier curves showing mouse survival. The log-rank (Mantel-Cox) test was applied to analyze mouse survival curve. **C:** Analysis of liver weight of the indicated mice at late stage (9.0 to 20.0 w.p.i). Data were analyzed by unpaired *t*-test. **D:** Representative gross images and H&E of livers from the mice. $n = 4$ mice with YAP/sgApc/pT3 plasmids (**A**); $n = 6$ mice with YAP/sgApc/dnTCF4 plasmids (**A**). $^*P < 0.05$, $^{**}P < 0.01$. Scale bars = 500 μm. Original magnification, ×40. H&E, hematoxylin and eosin; w.p.i, weeks post-injection.

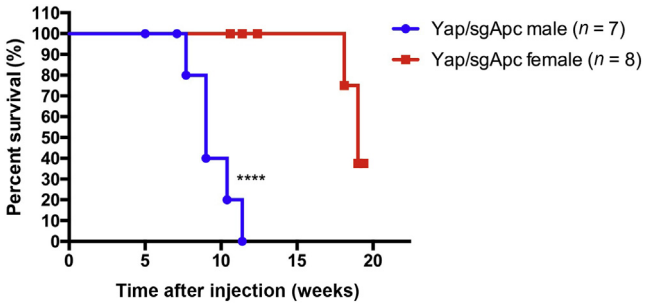


**Figure 12** Tumor progression is sex-dependent in Yap/sgApc mice. Kaplan-Meier survival curve of Yap/sgApc male and female mice. The log-rank (Mantel-Cox) test was applied to analyze mice survival. ****$P < 0.0001$ versus Yap/sgApc female.

deletion and hydrodynamic gene delivery. Thus, these data suggest that deletion of Apc in a small percentage of mouse hepatocytes, which might recapitulate more faithfully the human situation, is insufficient to trigger liver tumorigenesis. The results are consistent with these and other data showing that the GOF *Ctnnb1* mutation is unable to promote HCC development when activated in sporadic hepatocytes in the mouse liver.[40,41] Taken together, this body of evidence demonstrates that activation of the Wnt/β-catenin cascade via either GOF *Ctnnb1* mutation or LOF *APC* mutation is unable to promote HCC formation *in vivo*, and a second signal cooperating with activated Wnt/β-catenin is required to drive hepatocarcinogenesis. Consistent with this hypothesis, the loss of Apc was observed to synergize with additional activated oncogenes, such as Yap, Taz, and c-Met to produce liver malignant transformation in mice.

Interestingly, APC expression was induced in Yap/β-catenin tumors when compared with normal liver tissues, but not induced in Taz- or c-Met–driven tumors (Figure 9A and Supplemental Figure S2). We previously analyzed YAP target genes in human HCC cell lines[51] and found that silencing of YAP resulted in decreased APC expression in three of the four HCC cell lines examined here (Supplemental Figure S14A). In addition, analysis of the expression of APC and YAP pathway genes (*YAP1*, *JAG1*, *NOTCH2*, and *AMOTL2*) in the TCGA LIHC dataset indicated a positive correlation between APC mRNA expression and YAP pathway gene expression (Supplemental Figure S14B). Altogether, these data suggest that APC might be a YAP target in HCC. Additional studies are required to delineate the molecular crosstalk between APC and YAP in liver tumor development.

APC is an essential component of the β-catenin destruction complex, whose deletion enhances the stability of β-catenin, resulting in β-catenin nuclear translocation and activation.[11] Thus, the activation status of β-catenin in Yap/sgApc, Taz/sgApc, and c-Met/sgApc liver tumors was investigated, and as expected, the lesions from the three mouse models displayed cytoplasmic and/or nuclear staining for β-catenin and its downstream target GLUL, implying a high β-catenin activation in these tumors. Functionally, *Ctnnb1* conditional KO mice or overexpressing dnTCF4 provided convincing evidence that LOF *APC* mutation-driven liver tumor development requires an intact β-catenin/TCF4 signaling. These findings strongly suggest that therapeutic approaches aimed at targeting β-catenin/TCF4, including the use of lipid nanoparticles with siRNA against *CTNNB1* or soluble drugs such as tankyrase inhibitors,[62] might be effective for the treatment of liver tumors with LOF *APC* mutations. Additional studies will be required to further investigate the therapeutic efficacy of these approaches, and the mouse liver tumor models described in this study represent an excellent preclinical tool for these translational studies.

An intriguing finding from the present study is that, although mouse liver tumors induced by sgApc or GOF *Ctnnb1* mutations share multiple molecular and histologic features, they also have some differences. For instance, whereas Yap/β-catenin liver tumor lesions emerged and progressed with features of human fetal type HB, virtually identical lesions developing in Yap/sgApc and Taz/sgApc differentiated into HCC-like lesions in the late stage of carcinogenesis. We have previously shown that Taz/β-catenin mice develop HB-like tumors characterized by both epithelial and mesenchymal features.[37] Different from the Taz/β-catenin model, both HB-like and HCC-like lesions developing in Taz/sgApc mice did not exhibit the presence of a mesenchymal component. Sex differences have been clearly documented in many tumor types. Males have a higher incidence and mortality than females in many cancer types, including liver cancer.[63,64] There is a growing body of evidence supporting sex differences in cancers revealed by cancer genomic studies.[65] A pan-cancer analysis of 1983 tumors of 28 subtypes uncovered sex differences in driver gene mutation frequencies. For instance, *CTNNB1* mutation frequency in HCC presented a significant sex difference, with more male patients harboring *CTNNB1* mutations than female patients (male: 31%, female: 13%). These sex differences in oncogenic mutational processes might indicate differences in tumor origin and trajectories between male and female patients.[66] As per a recent study, *APC* mutant HB is enriched in males, with 83% of *APC* mutation patients with HB and 58% of all patients with HB are male.[22] Here, preliminary data indicate that liver tumor development driven by the combination of Apc loss and Yap or Taz activation is influenced by the mouse's sex. These results suggest that LOF *APC* mutation differentially contributes to liver tumor pathogenesis in a sex-biased manner. The possible mechanisms leading to this event are unknown and might include a different path by which APC regulates metabolism, angiogenesis, immunity, or epigenetics, in males and females.[67] However, additional studies are required to investigate these possible mechanisms.

Overexpression of oncogenes in the mouse liver depleted of Apc resulted in tumor lesions that differred

depending on the oncogenes injected. Indeed, although HB-like tumors finally evolving into HCC were detected in Yap/sgApc and Taz/sgApc mice, liver lesions developing in c-Met/sgApc mice consisted of pure HCC cells from the beginning. At the molecular level, these histopathologic differences were associated with the relocalization of β-catenin to the cytoplasm and membrane of tumor cells in the advanced (HCC) lesions, as well as by the increased expression of markers of mature hepatocytes (HNF4α, CEBPα) and lipogenesis (FASN, SCD1) and the down-regulation of the progenitor marker SOX9 in Yap/sgApc and Taz/sgApc mice. Intriguingly, tumors developing in Yap/β-catenin and Taz/β-catenin mice do not show a similar HB to HCC conversion even in the advanced stages of carcinogenesis, further underlining the existence of differences in the effects of Apc loss and mutant β-catenin activation. The histopathologic divergences were mirrored by differences at protein and mRNA levels in tumors generated by either loss of Apc or β-catenin activation. Specifically, a subset of β-catenin targets was more expressed in sgApc models, whereas the levels of some members of the Notch pathway were significantly higher in β-catenin mutant tumors. In particular, GLUL and its downstream effector mTOR were more homogeneously expressed in the lesions generated in Apc-depleted mice than in corresponding tumors from β-catenin mutant mice, where a scattered and discontinuous immunoreactivity for the same proteins was observed. Based on these findings, it would be highly interesting to investigate whether sgApc and β-catenin mutant tumors respond differently or similarly to mTOR inhibitors, such as rapamycin and rapalogs. Moreover, additional studies should be conducted with more comprehensive approaches (transcriptomics, proteomics) to determine the whole spectrum of molecular differences in sgApc and β-catenin mutant models, as well as to identify the key genes responsible for the observed dissimilarities. Nonetheless, it must be emphasized that tumors on a sgAPc and β-catenin mutant background displayed a similar tumor latency and burden, as well as an analogous overall survival, thus implying that tumorigenesis is similar in these mouse models.

In summary, data from the current study indicate that APC inactivation or down-regulation occurs in a subset of human HCC and HB patients. Loss of Apc in mice cooperates with canonical liver oncogenes to induce hepatic tumors that develop only in the presence of intact β-catenin/TCF4 signaling. Tumors generated in Apc-depleted mice show similarities and differences at the histomorphologic and molecular level when compared with those developing in the context of a β-catenin–activating mutation. Treatment with mTOR and/or Wnt/β-catenin inhibitors might be beneficial for HCC patients displaying inactivating mutations of *APC*.

## Acknowledgment

We thank Dr. Wen Xue (University of Massachusetts Medical School, Worcester, MA) for sharing the sgApc plasmids.

## Authors Contributions

Y.Z. executed this study and wrote the manuscript; B.L. assisted in maintenance of *Ctnnb1*$^{f/f}$ mice; X.S. assisted with RNA extraction from mouse liver tissues; H.W. assisted with APC data analysis; M.E. performed immunohistochemistry for molecular characterization of liver tumors and evaluated the mouse lesions at the histopathologic level; Y.Z. assisted with hydrodynamic injection; L.T. proofread the manuscript; D.F.C. and X.C. supervised the study and edited the manuscript.

## Supplemental Data

Supplemental material for this article can be found at *http://doi.org/10.1016/j.ajpath.2021.01.010*.

## References

1. Torre LA, Bray F, Siegel RL, Ferlay J, Lortet-Tieulent J, Jemal A: Global cancer statistics, 2012. CA Cancer J Clin 2015, 65:87–108
2. Darbari A, Sabin KM, Shapiro CN, Schwarz KB: Epidemiology of primary hepatic malignancies in U.S. children. Hepatology 2003, 38:560–566
3. Wang W, Smits R, Hao H, He C: Wnt/beta-catenin signaling in liver cancers. Cancers 2019, 11:926
4. Bertuccio P, Turati F, Carioli G, Rodriguez T, La Vecchia C, Malvezzi M, Negri E: Global trends and predictions in hepatocellular carcinoma mortality. J Hepatol 2017, 67:302–309
5. López-Terrada D, Alaggio R, de Dávila MT, Czauderna P, Hiyama E, Katzenstein H, Leuschner I, Malogolowkin M, Meyers R, Ranganathan S, Tanaka Y, Tomlinson G, Fabrè M, Zimmermann A, Finegold MJ; Children's Oncology Group Liver Tumor Committee: Towards an international pediatric liver tumor consensus classification: proceedings of the Los Angeles COG liver tumors symposium. Mod Pathol 2014, 27:472–491
6. Clevers H, Nusse R: Wnt/beta-catenin signaling and disease. Cell 2012, 149:1192–1205
7. Willert K, Jones KA: Wnt signaling: is the party in the nucleus? Genes Dev 2006, 20:1394–1404
8. Perugorria MJ, Olaizola P, Labiano I, Esparza-Baquer A, Marzioni M, Marin JJG, Bujanda L, Banales JM: Wnt-beta-catenin signalling in liver development, health and disease. Nat Rev Gastroenterol Hepatol 2019, 16:121–136
9. Mavila N, Thundimadathil J: The emerging roles of cancer stem cells and Wnt/beta-catenin signaling in hepatoblastoma. Cancers 2019, 11:1406
10. Forbes SA, Beare D, Boutselakis H, Bamford S, Bindal N, Tate J, Cole CG, Ward S, Dawson E, Ponting L, Stefancsik R, Harsha B, Kok CY, Jia M, Jubb H, Sondka Z, Thompson S, De T, Campbell PJ: COSMIC: somatic cancer genetics at high-resolution. Nucleic Acids Res 2017, 45:D777–D783
11. Valvezan AJ, Zhang F, Diehl JA, Klein PS: Adenomatous polyposis coli (APC) regulates multiple signaling pathways by enhancing

glycogen synthase kinase-3 (GSK-3) activity. J Biol Chem 2012, 287: 3823−3832
12. De Queiroz Rossanese LB, De Lima Marson FA, Ribeiro JD, Coy CS, Bertuzzo CS: APC germline mutations in families with familial adenomatous polyposis. Oncol Rep 2013, 30:2081−2088
13. Paulson S, Patel C, Patel H: From the gut to the liver: another organ to watch in FAP patients. Case Rep Pathol 2016, 2016:1738696
14. Yang A, Sisson R, Gupta A, Tiao G, Geller JI: Germline APC mutations in hepatoblastoma. Pediatr Blood Cancer 2018, 65:e26892
15. Aretz S, Koch A, Uhlhaas S, Friedl W, Propping P, von Schweinitz D, Pietsch T: Should children at risk for familial adenomatous polyposis be screened for hepatoblastoma and children with apparently sporadic hepatoblastoma be screened for APC germline mutations? Pediatr Blood Cancer 2006, 47:811−818
16. Hughes LJ, Michels VV: Risk of hepatoblastoma in familial adenomatous polyposis. Am J Med Genet 1992, 43:1023−1025
17. Fearnhead NS, Britton MP, Bodmer WF: The ABC of APC. Hum Mol Genet 2001, 10:721−733
18. Lin Y, Wu Z, Guo W, Li J: Gene mutations in gastric cancer: a review of recent next-generation sequencing studies. Tumour Biol 2015, 36: 7385−7394
19. Nagase H, Nakamura Y: Mutations of the APC (adenomatous polyposis coli) gene. Hum Mutat 1993, 2:425−434
20. Katoh M: Multi-layered prevention and treatment of chronic inflammation, organ fibrosis and cancer associated with canonical WNT/beta-catenin signaling activation (Review). Int J Mol Med 2018, 42:713−725
21. Guichard C, Amaddeo G, Imbeaud S, Ladeiro Y, Pelletier L, Maad IB, Calderaro J, Bioulac-Sage P, Letexier M, Degos F, Clement B, Balabaud C, Chevet E, Laurent A, Couchy G, Letouze E, Calvo F, Zucman-Rossi J: Integrated analysis of somatic mutations and focal copy-number changes identifies key genes and pathways in hepatocellular carcinoma. Nat Genet 2012, 44:694−698
22. Morcrette G, Hirsch TZ, Badour E, Pilet J, Caruso S, Calderaro J, Martin Y, Imbeaud S, Letouzé E, Rebouissou S, Branchereau S, Taque S, Chardot C, Guettier C, Scoazec J-Y, Fabre M, Brugières L, Zucman-Rossi J: APC germline hepatoblastomas demonstrate cisplatin-induced intratumor tertiary lymphoid structures. Oncoimmunology 2019, 8:e1583547
23. Yu FX, Zhao B, Guan KL: Hippo pathway in organ size control, tissue homeostasis, and cancer. Cell 2015, 163:811−828
24. Kodaka M, Hata Y: The mammalian Hippo pathway: regulation and function of YAP1 and TAZ. Cell Mol Life Sci 2015, 72:285−306
25. Lin KC, Park HW, Guan KL: Regulation of the Hippo pathway transcription factor TEAD. Trends Biochem Sci 2017, 42:862−872
26. Zhang S, Zhou D: Role of the transcriptional coactivators YAP/TAZ in liver cancer. Curr Opin Cell Biol 2019, 61:64−71
27. Patel SH, Camargo FD, Yimlamai D: Hippo signaling in the liver regulates organ size, cell fate, and carcinogenesis. Gastroenterology 2017, 152:533−545
28. Li H, Wolfe A, Septer S, Edwards G, Zhong X, Abdulkarim AB, Ranganathan S, Apte U: Deregulation of Hippo kinase signalling in human hepatic malignancies. Liver Int 2012, 32:38−47
29. Hu J, Che L, Li L, Pilo MG, Cigliano A, Ribback S, Li X, Latte G, Mela M, Evert M, Dombrowski F, Zheng G, Chen X, Calvisi DF: Co-activation of AKT and c-Met triggers rapid hepatocellular carcinoma development via the mTORC1/FASN pathway in mice. Sci Rep 2016, 6:20484
30. Wang H, Rao B, Lou J, Li J, Liu Z, Li A, Cui G, Ren Z, Yu Z: The function of the HGF/c-Met axis in hepatocellular carcinoma. Front Cell Dev Biol 2020, 8:55
31. Organ SL, Tsao MS: An overview of the c-MET signaling pathway. Ther Adv Med Oncol 2011, 3:S7−S19
32. Garcia-Vilas JA, Medina MA: Updates on the hepatocyte growth factor/c-Met axis in hepatocellular carcinoma and its therapeutic implications. World J Gastroenterol 2018, 24:3695−3708
33. Bouattour M, Raymond E, Qin S, Cheng AL, Stammberger U, Locatelli G, Faivre S: Recent developments of c-Met as a therapeutic target in hepatocellular carcinoma. Hepatology 2018, 67:1132−1149
34. Fasolo A, Sessa C, Gianni L, Broggini M: Seminars in clinical pharmacology: an introduction to MET inhibitors for the medical oncologist. Ann Oncol 2013, 24:14−20
35. Xin Y, Jin D, Eppler S, Damico-Beyer LA, Joshi A, Davis JD, Kaur S, Nijem I, Bothos J, Peterson A, Patel P, Bai S: Population pharmacokinetic analysis from phase I and phase II studies of the humanized monovalent antibody, onartuzumab (MetMAb), in patients with advanced solid tumors. J Clin Pharmacol 2013, 53:1103−1111
36. Boccaccio C, Comoglio PM: Invasive growth: a MET-driven genetic programme for cancer and stem cells. Nat Rev Cancer 2006, 6: 637−645
37. Zhang S, Zhang J, Evert K, Li X, Liu P, Kiss A, Schaff Z, Ament C, Zhang Y, Serra M, Evert M, Chen N, Xu F, Chen X, Tao J, Calvisi DF, Cigliano A: The Hippo effector transcriptional coactivator with PDZ-binding motif cooperates with oncogenic beta-catenin to induce hepatoblastoma development in mice and humans. Am J Pathol 2020, 190:1397−1413
38. Lee SA, Ho C, Roy R, Kosinski C, Patil MA, Tward AD, Fridlyand J, Chen X: Integration of genomic analysis and in vivo transfection to identify sprouty 2 as a candidate tumor suppressor in liver cancer. Hepatology 2008, 47:1200−1210
39. Patil MA, Lee SA, Macias E, Lam ET, Xu C, Jones KD, Ho C, Rodriguez-Puebla M, Chen X: Role of cyclin D1 as a mediator of c-Met- and beta-catenin-induced hepatocarcinogenesis. Cancer Res 2009, 69:253−261
40. Tao J, Xu E, Zhao Y, Singh S, Li X, Couchy G, Chen X, Zucman-Rossi J, Chikina M, Monga SPS: Modeling a human hepatocellular carcinoma subset in mice through coexpression of met and point-mutant beta-catenin. Hepatology 2016, 64: 1587−1605
41. Tward AD, Jones KD, Yant S, Cheung ST, Fan ST, Chen X, Kay MA, Wang R, Bishop JM: Distinct pathways of genomic progression to benign and malignant tumors of the liver. Proc Natl Acad Sci U S A 2007, 104:14771−14776
42. Chen X, Calvisi DF: Hydrodynamic transfection for generation of novel mouse models for liver cancer research. Am J Pathol 2014, 184: 912−923
43. Cancer Genome Atlas Research Network: Comprehensive and integrative genomic characterization of hepatocellular carcinoma. Cell 2017, 169:1327−1341.e23
44. Calvisi DF, Ladu S, Gorden A, Farina M, Lee JS, Conner EA, Schroeder I, Factor VM, Thorgeirsson SS: Mechanistic and prognostic significance of aberrant methylation in the molecular pathogenesis of human hepatocellular carcinoma. J Clin Invest 2007, 117:2713−2722
45. Villanueva A, Portela A, Sayols S, Battiston C, Hoshida Y, Mendez-Gonzalez J, Imbeaud S, Letouze E, Hernandez-Gea V, Cornella H, Pinyol R, Sole M, Fuster J, Zucman-Rossi J, Mazzaferro V, Esteller M, Llovet JM; HEPTROMIC Consortium: DNA methylation-based prognosis and epidrivers in hepatocellular carcinoma. Hepatology 2015, 61:1945−1956
46. Koch A, De Meyer T, Jeschke J, Van Criekinge W: MEXPRESS: visualizing expression, DNA methylation and clinical TCGA data. BMC Genomics 2015, 16:636
47. Sumazin P, Chen Y, Trevino LR, Sarabia SF, Hampton OA, Patel K, Mistretta TA, Zorman B, Thompson P, Heczey A, Comerford S, Wheeler DA, Chintagumpala M, Meyers R, Rakheja D, Finegold MJ, Tomlinson G, Parsons DW, Lopez-Terrada D: Genomic analysis of hepatoblastoma identifies distinct molecular and prognostic subgroups. Hepatology 2017, 65:104−121
48. Qiao Y, Wang J, Karagoz E, Liang B, Song X, Shang R, Evert K, Xu M, Che L, Evert M, Calvisi DF, Tao J, Wang B, Monga SP, Chen X: Axis inhibition protein 1 (Axin1) deletion-induced

hepatocarcinogenesis requires intact beta-catenin but not Notch cascade in mice. Hepatology 2019, 70:2003−2017
49. Perra A, Kowalik MA, Ghiso E, Ledda-Columbano GM, Di Tommaso L, Angioni MM, Raschioni C, Testore E, Roncalli M, Giordano S, Columbano A: YAP activation is an early event and a potential therapeutic target in liver cancer development. J Hepatol 2014, 61:1088−1096
50. Hilman D, Gat U: The evolutionary history of YAP and the hippo/-YAP pathway. Mol Biol Evol 2011, 28:2403−2417
51. Wang H, Wang J, Zhang S, Jia J, Liu X, Zhang J, Wang P, Song X, Che L, Liu K, Ribback S, Cigliano A, Evert M, Wu H, Calvisi DF, Zeng Y, Chen X: Distinct and overlapping roles of Hippo effectors YAP and TAZ during human and mouse hepatocarcinogenesis. Cell Mol Gastroenterol Hepatol 2020, 11:1095−1117
52. Tao J, Calvisi DF, Ranganathan S, Cigliano A, Zhou L, Singh S, Jiang L, Fan B, Terracciano L, Armeanu-Ebinger S, Ribback S, Dombrowski F, Evert M, Chen X, Monga SPS: Activation of beta-catenin and Yap1 in human hepatoblastoma and induction of hepatocarcinogenesis in mice. Gastroenterology 2014, 147: 690−701
53. Shang R, Song X, Wang P, Zhou Y, Lu X, Wang J, Xu M, Chen X, Utpatel K, Che L, Liang B, Cigliano A, Evert M, Calvisi DF, Chen X: Cabozantinib-based combination therapy for the treatment of hepatocellular carcinoma. Gut 2020, [Epub ahead of print] doi: 10.1136/gutjnl-2020-320716
54. Calvisi DF: [De novo lipogenesis: role in hepatocellular carcinoma]. German. Pathologe 2011, 32(Suppl 2):174−180
55. Hankey W, Frankel WL, Groden J: Functions of the APC tumor suppressor protein dependent and independent of canonical WNT signaling: implications for therapeutic targeting. Cancer Metastasis Rev 2018, 37:159−172
56. Jewell JL, Kim YC, Russell RC, Yu F-X, Park HW, Plouffe SW, Tagliabracci VS, Guan K-L: Metabolism. Differential regulation of mTORC1 by leucine and glutamine. Science 2015, 347: 194−198
57. Adebayo Michael AO, Ko S, Tao J, Moghe A, Yang H, Xu M, Russell JO, Pradhan-Sundd T, Liu S, Singh S, Poddar M, Monga JS, Liu P, Oertel M, Ranganathan S, Singhi A, Rebouissou S, Zucman-Rossi J, Ribback S, Calvisi D, Qvartskhava N, Görg B, Häussinger D, Chen X, Monga SP: Inhibiting glutamine-dependent mTORC1 activation ameliorates liver cancers driven by beta-catenin mutations. Cell Metab 2019, 29:1135−1150.e6
58. Yan M, Li G, An J: Discovery of small molecule inhibitors of the Wnt/beta-catenin signaling pathway by targeting beta-catenin/Tcf4 interactions. Exp Biol Med (Maywood) 2017, 242:1185−1197
59. Tao J, Zhang R, Singh S, Poddar M, Xu E, Oertel M, Chen X, Ganesh S, Abrams M, Monga SP: Targeting beta-catenin in hepatocellular cancers induced by coexpression of mutant beta-catenin and K-Ras in mice. Hepatology 2017, 65:1581−1599
60. Aoki K, Taketo MM: Adenomatous polyposis coli (APC): a multi-functional tumor suppressor gene. J Cell Sci 2007, 120: 3327−3335
61. Colnot S, Decaens T, Niwa-Kawakita M, Godard C, Hamard G, Kahn A, Giovannini M, Perret C: Liver-targeted disruption of Apc in mice activates beta-catenin signaling and leads to hepatocellular carcinomas. Proc Natl Acad Sci U S A 2004, 101: 17216−17221
62. Ma L, Wang X, Jia T, Wei W, Chua M-S, So S: Tankyrase inhibitors attenuate WNT/beta-catenin signaling and inhibit growth of hepatocellular carcinoma cells. Oncotarget 2015, 6: 25390−25401
63. Edgren G, Liang L, Adami HO, Chang ET: Enigmatic sex disparities in cancer incidence. Eur J Epidemiol 2012, 27:187−196
64. Cook MB, McGlynn KA, Devesa SS, Freedman ND, Anderson WF: Sex disparities in cancer mortality and survival. Cancer Epidemiol Biomarkers Prev 2011, 20:1629−1637
65. Li CH, Haider S, Shiah Y-J, Thai K, Boutros PC: Sex differences in cancer driver genes and biomarkers. Cancer Res 2018, 78: 5527−5537
66. Li CH, Prokopec SD, Sun RX, Yousif F, Schmitz N, Subtypes PT, PCAWG Tumour Subtypes and Clinical Translation, Boutros PC, PCAWG Consortium: Sex differences in oncogenic mutational processes. Nat Commun 2020, 11:4330
67. Rubin JB, Lagas JS, Broestl L, Sponagel J, Rockwell N, Rhee G, Rosen SF, Chen S, Klein RS, Imoukhuede P, Luo J: Sex differences in cancer mechanisms. Biol Sex Differ 2020, 11:17